PHILIPS

Application book

PHILIPS

Electronic components and materials

Isolators and Circulators

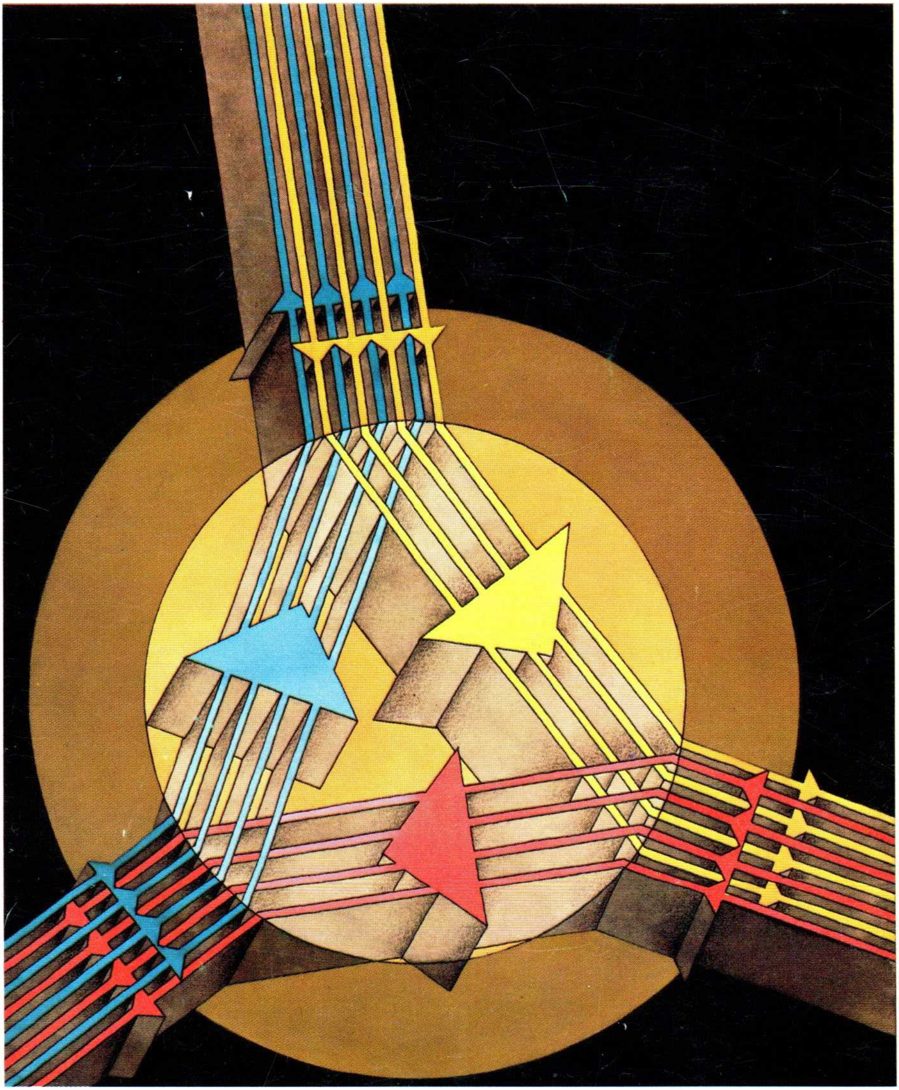

Isolators and Circulators

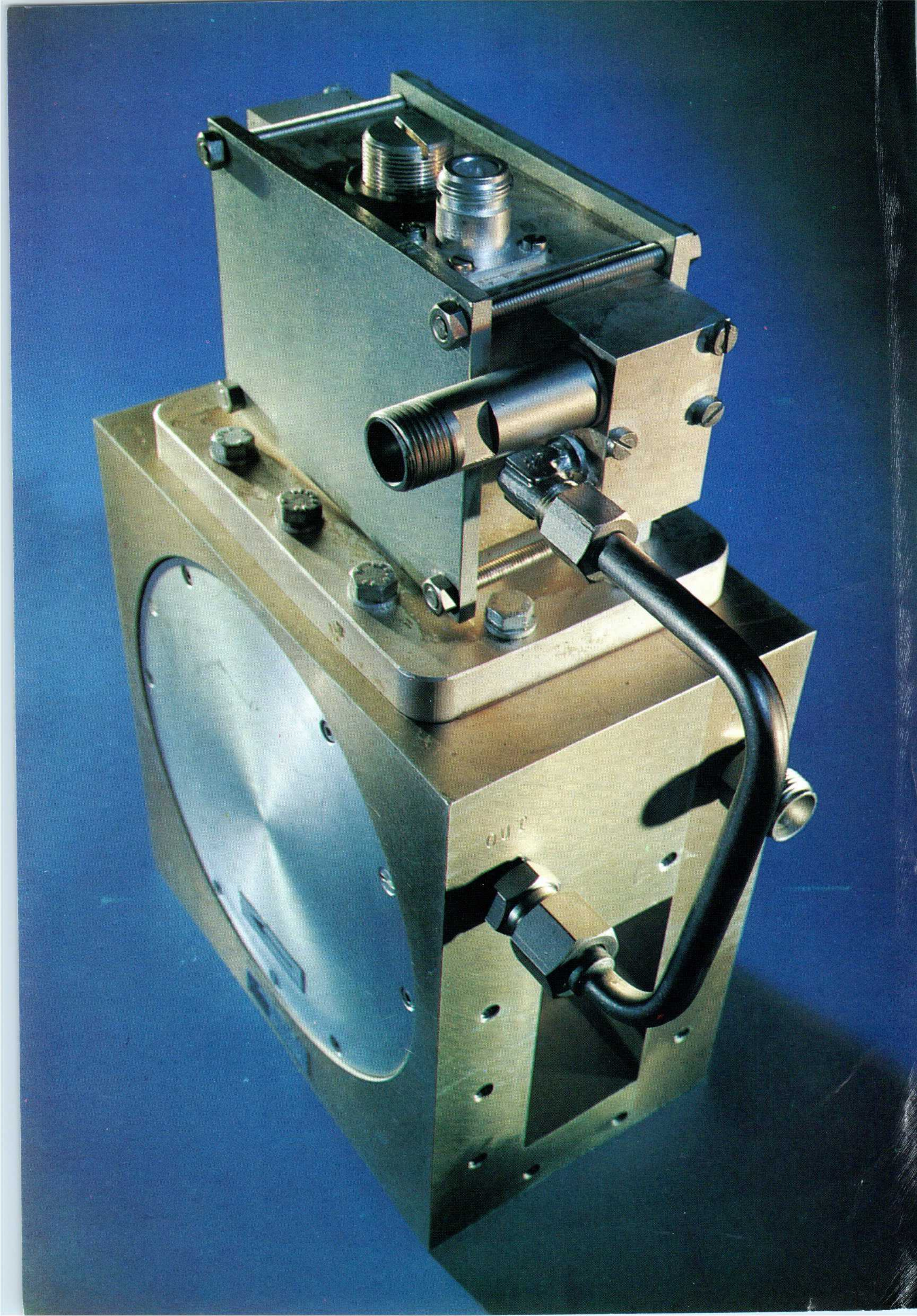
OUT

Isolators and Circulators

Edited by T. S. Christian

Elcoma Publications, Eindhoven

ELECTRONIC COMPONENTS AND MATERIALS DIVISION

Acknowledgement

Based upon "Einwegleitung, Zirkulatoren, Phasenschieber", January 1973 by G. Euler *), with F. Pötzl *), and L. van der Kint **), this edition has been substantially revised with further contributions from Mr. van der Kint, whose assistance the editor gratefully acknowledges.

Acknowledgement from original version:

"The Author wishes to express his thanks to Messrs W. Golombek, E. G. Metz and G. Voss for their invaluable guidance and support".

Frontispiece

A 6 kW isolator - connected circulator for microwave heating systems. This isolator is designed to optimize magnetron performance by removing the wide v.s.w.r. variations of the load from the magnetron output.

*) Valvo G.m.b.H. Hamburg, Germany.

**) N.V. Philips' Gloeilampenfabrieken, Eindhoven, The Netherlands.

Contents

Useful design data in this publication

Graphs

Nomograms and scales

1 Introducing the devices

Isolators and circulators are key elements in modern u.h.f. and microwave engineering. Their fundamental property of non-reciprocity is capable of simplifying the construction and improving the stability and efficiency of radar and communication systems. Similarly, equipments used in the development and testing of such systems can usually be improved in accuracy and convenience of operation by including isolators or circulators in their input or output circuits.

The principal application which the isolator finds is the isolation of a source from its load. In the case of an amplifier which might be affected or even damaged by power reflected back from the load, the inclusion of an isolator between output and load is a worthwhile improvement and safeguard.

Circulators are used in two basic ways. Three-port circulators, the usual form, are frequently employed as high-power isolators, reflected power being absorbed in a load connected to its third port. Additionally, they may be used to enable two or more transmitters to share the same aerial, or to allow the use of a single aerial for simultaneous transmission and reception. Frequency multiplexing is easily and effectively accomplished with suitable networks of circulators and filters. Single terminal (reflection) amplifiers, such as the parametric amplifier, depend for their successful operation on circulators. By replacing the fixed load of an isolator-connected circulator by a variable load or variable length short circuit, adjustable attenuators or phase shifting elements capable of handling high powers are readily realizable.

Isolators and circulators are both electronic components which do not show reciprocity; that is, they are examples of the gyrator. Their properties depend on the direction of flow of electromagnetic energy through them. Both devices are passive circuit elements, the directional properties being due to the interaction between the energy flowing and the electrons in magnetically biased soft ferrimagnetic material, usually a ferrite.

Figure 1 shows a typical isolator with its symbol. An ideal device would pass all the energy supplied to port *1*, but absorb all the energy supplied to port *2*. This principle is illustrated rather dramatically in Fig. 2.

The circulator, Fig. 3, would, under ideal conditions and with properly matched (reflection-free) terminations on all ports, permit coupling only between adjacent ports in one direction. Thus, energy entering port *1* would leave only by port *2*; energy entering port *2* would leave only by port *3* and so on. Again, this principle could have its parallel in road traffic engineering, see Fig. 4.

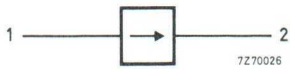

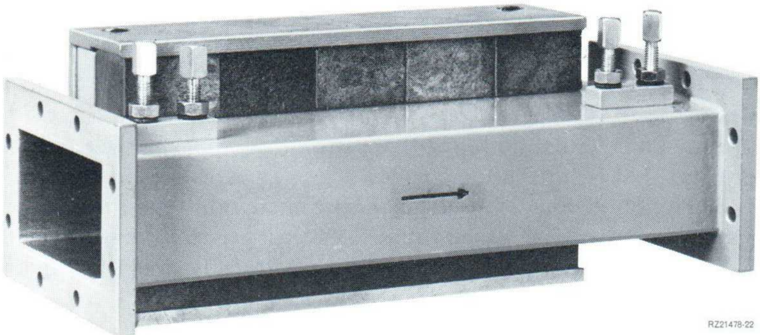

Fig. 1 Common design of a waveguide isolator together with the symbol usually employed to represent the isolator function.

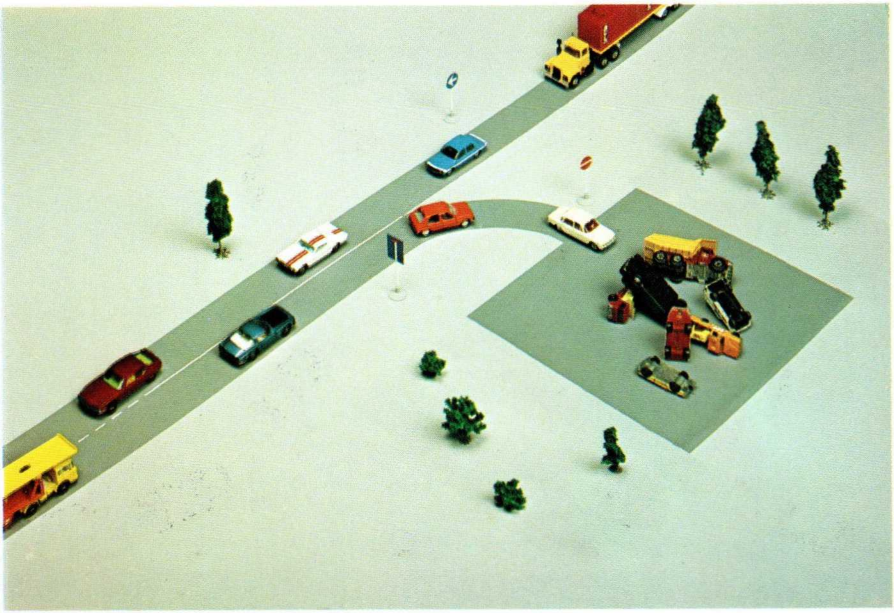

Fig. 2 It would seem that the isolator principle is capable of solving traffic congestion problems!

Fig. 3 Co-axial type of circulator, together with the usual symbol for a circulator.

740829-07-01

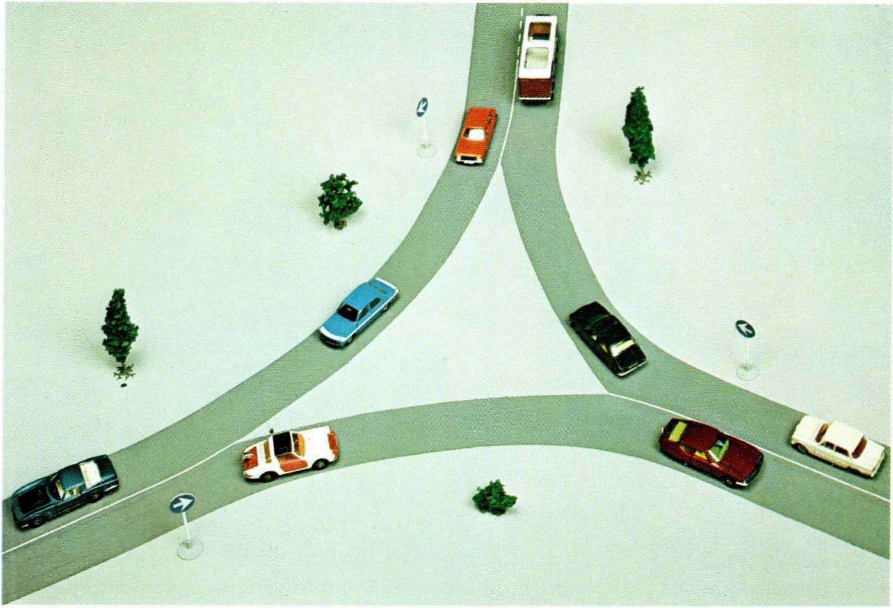

Fig. 4 Anyone who has lost his way on modern motorways can believe that traffic engineers have discovered the circulator principle!

To gain an insight into the operating principle of non-reciprocal components such as isolators, and circulators, it is first necessary to discuss the behaviour of the ferrite, the principal element in a combination of static and alternating fields. Ferrites are magnetic materials with excellent insulation properties. Because of their low conductivity they can be used in h.f. applications, eddy current losses being negligible.

Like ferromagnetic materials, ferrites consist of magnetic domains (Fig. 5), called Weiss domains after their discoverer. They may be anywhere between 1 and 100 μm across. The individual domains are separated from each other by Bloch walls. Their inherent magnetization results from mutual exchange effects between electron spins. With no external magnetic field applied, the individual domains are randomly oriented, so that the net resultant magnetization is zero.

When a sufficiently strong magnetic field is applied, the magnetic moments of the individual domains are oriented with the direction of the field, and wall displacements take place. When this happens, the domains aligned with the external field expand at the expense of others which have a different orientation. This process is not a simple switching process because the magnetization originates from the electron spins within the domains. Thus each domain can be

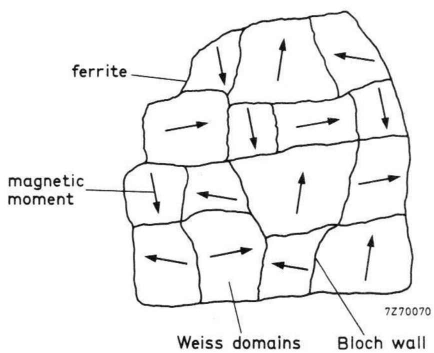

Fig. 5 Terminology used in explaining the properties of a ferrite material.

regarded as a spinning top with a precessing axis. During the precession one such top is turned through 90°, performing a damped precessional motion.

In a ferrite material the precessional motion is around the direction of the external magnetic field. Once the precession has stopped, the directions of the external field and the rotated magnetic moments of the Weiss domains are the same. If, as shown in Fig. 6, an alternating field of suitable frequency is applied perpendicular to the static field, the precession around the H_i-field continues. The magnetic moment M precesses around the direction H_i.

Whether external magnetic fields are applied in the y- or z-direction, one component of the magnetic moment will be operative in the x-direction (M_x in Fig. 6). Now the relationship between induction and magnetic field, $B = \mu H$ can no longer be depicted as a μ-scale, but rather by a linear system of vectors

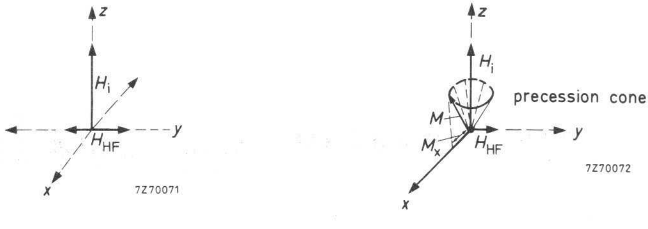

(a) (b)

Fig. 6 Terms and coordinate system used in the description of precession.

that can be written as a tensor, known as the Polder tensor [1]. The relationship between B and H is thus

$$B_x = \mu H_x - \mathrm{j}\varkappa H_y$$
$$B_y = \mathrm{j}\varkappa H_x + \mu H_y$$
$$B_z = \mu_0 H_z$$

or expressed in the form of a tensor

$$\begin{pmatrix} B_x \\ B_y \\ B_z \end{pmatrix} = \mu_0 \begin{pmatrix} \mu & -\mathrm{j}\varkappa & 0 \\ \mathrm{j}\varkappa & \mu & 0 \\ 0 & 0 & \mu_0 \end{pmatrix} \begin{pmatrix} H_x \\ H_y \\ H_z \end{pmatrix}.$$

The value of the induction component perpendicular to the magnetic a.c. field is determined by the value of $\varkappa$. The quantities $\mu = \mu' - \mathrm{j}\mu''$ and $\varkappa = \varkappa' - \mathrm{j}\varkappa''$ are complex and depend on the static magnetic field, the frequency, and the material properties of the ferrite.

If the magnetic plane of an electromagnetic wave is parallel to H_i, the relative permeability is ($\mu_{\mathrm{eff}\,||} = \mu_0$), since the ferrite is always saturated. The propagation speed is $\gamma = \mathrm{j}\omega\sqrt{\varepsilon\mu_0}$, hence the ferrite has no gyromagnetic effect on the wave.

Where the magnetic plane of the electromagnetic wave is perpendicular to H_i,

$$\mu_{\mathrm{eff}\perp} = (\mu^2 - \varkappa^2)/\mu.$$ [1]

(Here the propagation constant is $\gamma = \mathrm{j}\omega\sqrt{\varepsilon\mu_{\mathrm{eff}\perp}}$.) Fig. 7 shows how the real and imaginary parts of $\mu_{\mathrm{eff}\,|}$ and of $\mu_{\mathrm{eff}\,||}$ vary as functions of H_i.

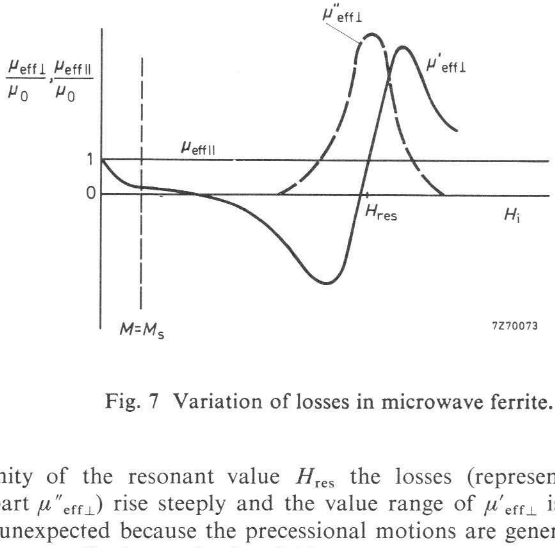

Fig. 7 Variation of losses in microwave ferrite.

In the vicinity of the resonant value H_{res} the losses (represented by the imaginary part $\mu''_{eff\perp}$) rise steeply and the value range of $\mu'_{eff\perp}$ is expanded. This is not unexpected because the precessional motions are generated by the components perpendicular to the d.c. field.

With non-reciprocal components, the behaviour of the ferrite under the influence of the circularly polarized magnetic fields is of prime importance. A linearly polarized a.c. magnetic field can be regarded as consisting of two circular fields rotating in opposite directions. Thus two different permeability values may be obtained; for the field polarized clockwise (+) and for the field polarized anti-clockwise (—) (seen in the direction of the field), whence $\mu_+ = \mu - \varkappa$ and $\mu_- = \mu + \varkappa$. The corresponding propagation speeds are $\gamma_+ = j\omega\sqrt{\varepsilon\mu_+}$ and $\gamma_- = j\omega\sqrt{\varepsilon\mu_-}$.

[1] Curves calculated for a planar wave propagated perpendicular to the d.c. field.

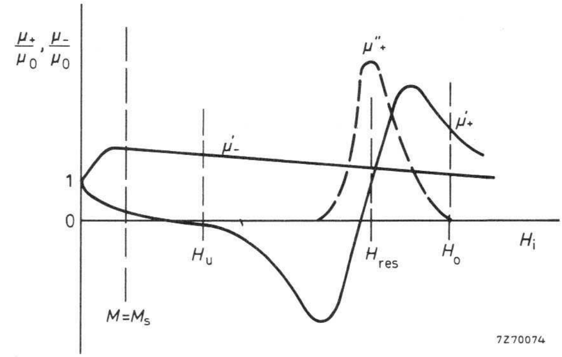

Fig. 8 Variation of μ''_+ with field, showing the resonant behaviour.

Fig. 8 illustrates[2] the real and the imaginary parts of the functions μ_+ and μ_- of the magnetic field[2]: μ_+ shows a distinct resonance behaviour, and a form resembling that of the curves $\mu_{\mathrm{eff}\perp}$ in Fig. 7. At resonance, losses are high, as is the value of the imaginary part μ''_+.

This behaviour can be interpreted as follows. At resonance the positively polarized wave causes the magnetic moments to precess around the d.c. field direction. The negatively polarized wave (—) counteracts precession, and so there can be no resonance.

[2] Curves calculated for a planar wave propagated parallel to the d.c. field.

2 Construction and operation

Non-reciprocal devices may be made by taking advantage of the resonance effects in ferrite. Directional behaviour is obtained by biasing a ferrite material with a steady magnetic field, when gyromagnetic effects occur during the interaction of electromagnetic energy with the ferrite, non-reciprocal properties being exhibited.

2.1 Waveguide isolators

Fig. 9 shows the construction of a waveguide-mounting isolator. Essentially, the device consists of a waveguide section with flanges; a thin ferrite bar is bonded along one of the narrow sides, slightly off-centre, the inwards facing surface of the ferrite being coated with a layer of some resistive material. An externally generated d.c. magnetic field, normal to the broad sides of the waveguide, biases the ferrite. Some means of adjustment, in this case tuning screws, is provided.

With such an arrangement, the electric field due to energy travelling in a direction determined by the sense of the biasing field, will be concentrated by the ferrite onto the resistive layer, and strong absorption will take place.

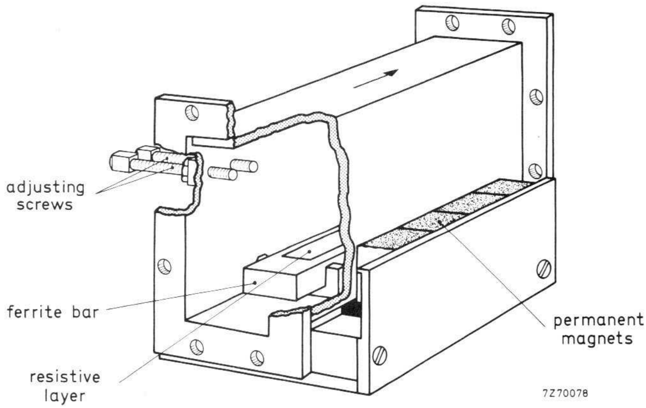

Fig. 9 Cut-away drawing of a waveguide isolator showing the principal constructional features.

Between the wall and the centre of a square waveguide containing an H_{01}-wave (magnetic fundamental wave), there are areas in which a magnetic a.c. field of rotating polarization occurs. Fig. 10*a* shows the field line pattern of the H_{01}-wave; Fig. 10*b* shows the magnetic field lines and the planes in which the rotating field is operative. The narrow side of the waveguide is perpendicular to the plane of drawing. If the wave travels from left to right, there will be a field rotating anti-clockwise above the centre of the waveguide, and a field rotating clockwise below the centre. If a strip of ferrite is introduced into this area, say at A, and if, furthermore, a sufficiently strong d.c. field is applied perpendicularly to the drawing plane in Fig. 10, the precessional motion will take place only if the h.f. wave travels from left to right through the waveguide. When this happens the energy of the wave is dissipated in the ferrite.

If the wave travels in the opposite direction, there will be no absorption in the ferrite rod or slab, because then the magnetic field rotates in the reveise direction and no resonance will take place (see Fig. 8).

This is the operating principle of "resonance" isolators which are widely used for narrow band applications. They have very high, isolation and fairly low insertion loss.

For wideband applications isolators are not usually driven at resonance, but far beyond. Then, the quantity μ''_+ determining the losses (Fig. 8) is still small, but μ'_+ is about unity, so that when energy is travelling from left to right in the figure, a concentration of field occurs in the ferrite, which is also due to the dielectric loading of the waveguide. This concentrated field (the electrical component) is absorbed by a resistive layer located on the ferrite strip, and thus the electromagnetic energy is dissipated as heat (see Fig. 4).

If the electromagnetic energy travels through the waveguide in the opposite direction (i.e. right to left in Fig. 10*a*), μ_{eff} will be negative, and the electric field will be excluded from the ferrite, producing a node in the field pattern. No energy will be dissipated in the resistive layer and there will be little loss.

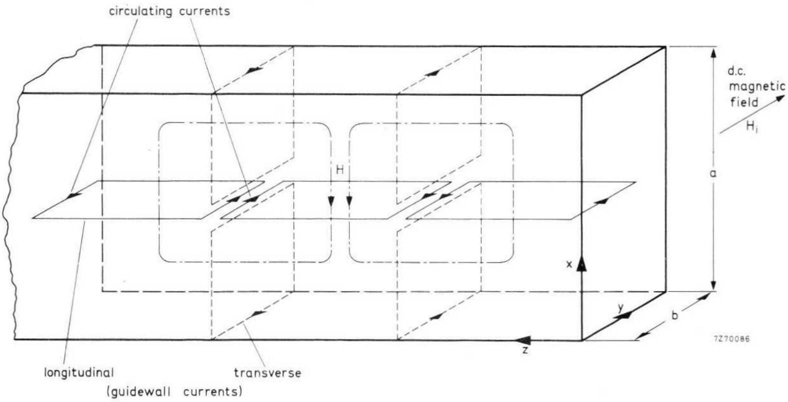

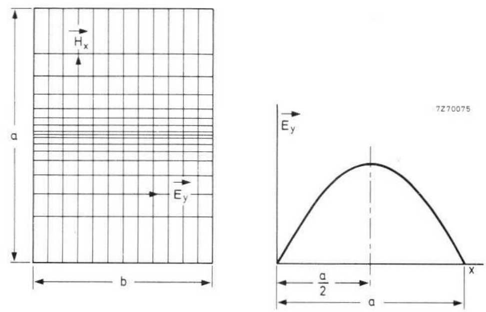

(a)

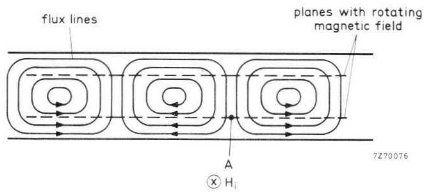

(b)

Fig. 10 Fields and currents associated with an H_{01}-wave (*a*) and the planes in which the field rotates (*b*).

2.2 Circulators

The basic structure of a waveguide circulator is shown in Fig. 11. A block of ferrite is mounted at the centre of a waveguide junction and biased with a steady magnetic field normal to the plane of the junction. The waveguide and the ferrite block are shaped to match the impedance of the connecting waveguide.

Circulators using tri-plate construction are also fairly simple, as illustrated by Fig. 12 with a 3-port Y-junction. Between the three conductor strips are two discs of ferrite biased by permanent magnets located above and below the junction. The striplines are equipped with matching elements – transmission line transformers or tuning screws and trimmers – and terminate in h.f. connectors.

The size of a circulator increases as its design operating frequency decreases, and at lower frequencies becomes impracticably large. Because of this, lumped circuit designs are used to produce compact designs. An example of this technique is shown in Fig. 13, where the conventional waveguide junction is replaced by three symmetrically coupled transmission line sections. Matching devices are not shown in this illustration.

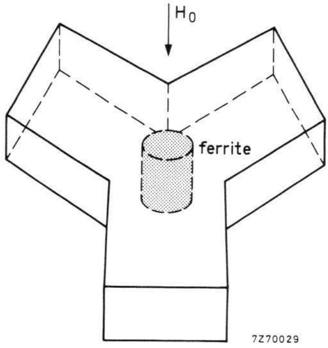

Fig. 11 Skeleton drawing of a waveguide circulator.

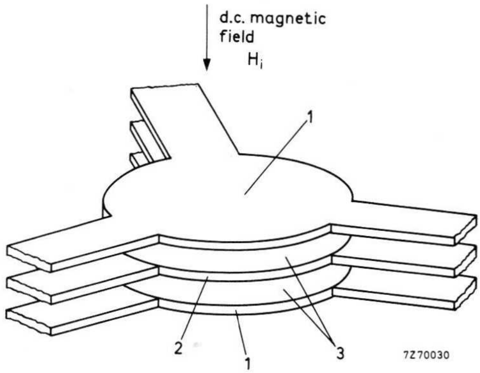

Fig. 12 Outline of a tri-plate circulator, ferrite discs (not shown) are located between the conductors.

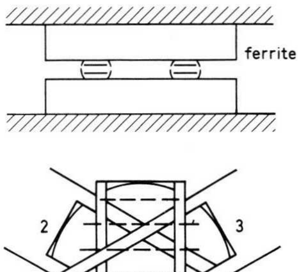

Fig. 13 To overcome the size problem associated with lower frequencies, lumped circuit elements may be used in circulator construction. In this example, symmetrically coupled transmission line sections are used.

The construction of a stripline circulator with ferrite discs and a guide branch was shown in Fig. 4. The field pattern of the fundamental electromagnetic oscillation for the disc-stripline structure is shown in Fig. 14. Let us first omit the d.c. field from consideration. The magnetic field vectors run parallel to the guide junction. The electric field is perpendicular to the ferrite discs and points alternately up and down in the various disc halves. At the centre there is a node line where the electric field disappears. If there is no magnetic field, equal amounts of energy reach the two remaining ports.

The h.f. field parallel to the guide junction can be regarded as resulting from the superposition of two polarized waves rotating in opposite directions.

If a d.c. magnetic field perpendicular to the junction is now applied, the two constituent waves have different permeability values: μ'_+ and μ'_-. This means that the two constituent waves rotate at different speeds. Consequently, depending on the d.c. field, the complete field pattern is shifted until, finally, the node points precisely towards one of the other ports. In Fig. 14 this is port *3*. The total amount of input power at port *1* is then guided to port *2*. Port *3* is decoupled, and the arrangement functions as a circulator.

The circulator has two operating points. It can be operated with d.c. fields either stronger or weaker than the resonance field. Both conditions are shown in Fig. 8 (values H_o and H_u).

In comparison with circulators operating below resonance, those operating above resonance require a stronger magnetic field. Consequently they are heavier and have a narrower bandwidth. They are only limited in power handling capability by internal arcing and heating, and have low losses. The power handling of circulators operating below resonance is limited by non-linear effects, and they have greater insertion losses which can in part be traced back to the incomplete saturation of individual parts of the ferrite.

This description of how the circulator operates can also be found in Fay and Comstock [2]. It is a particularly clear illustration. According to Bosma [3] the fields in the ferrite discs resulting from the interaction between h.f. fields and d.c. fields can be mathematically expressed in a progression. The calculation is very complex, and has, therefore, been omitted.

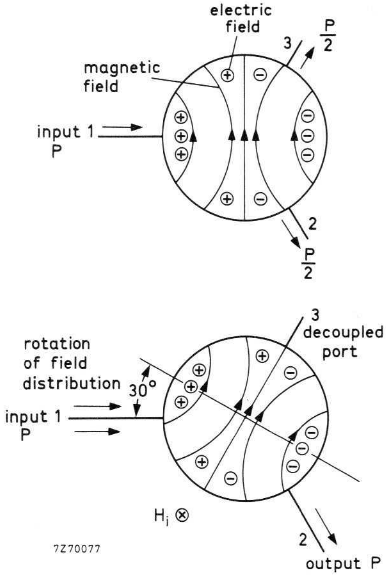

Fig. 14 Operating field pattern for the stripline circulator of Fig. 4.

RZ30190-3

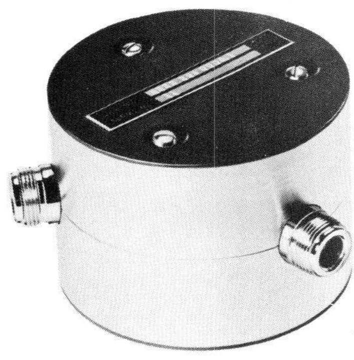

720717-08-03

Examples of coaxial circulators.

3 Characteristics

This section summarizes the more important characteristics of isolators and circulators, preparatory to discussing the practical applications of the devices themselves.

3.1 Isolators

The essential parameters of isolators are insertion loss and isolation.

Insertion loss (Fig. 15) is the proportion of power lost between the ports of the device when energy is travelling in the forward direction:

$$\text{insertion loss} = 10 \log \frac{\text{input power}}{\text{output power}} \ (\text{dB}).$$

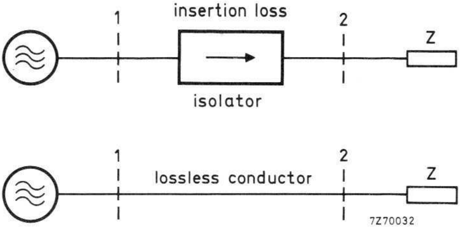

Fig. 15 With the lossless conductor, power levels at points *1* and *2* will be the same. When an isolator is inserted, these power levels differ by the insertion loss.

Thus it can be regarded as the attenuation resulting from the inclusion of the device in a transmission system. Insertion loss must be measured with the input and output of the isolator well matched.

Isolation (Fig. 16*a*) is the proportion of power lost between the ports of the device when energy is driven through it in the reverse direction:

$$\text{isolation} = 10 \log \frac{\text{input power}}{\text{output power}} \text{ (dB)}.$$

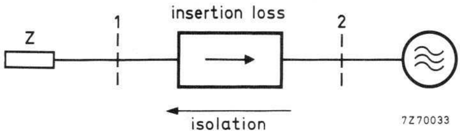

Fig. 16*a* Isolation may be regarded as the insertion loss of an isolator connected in reverse. Compare this drawing with Fig. 15.

As with insertion loss, isolation must be measured with matched terminations.

By way of an example, Fig. 16*b* gives the results of measurements of the frequency dependence of both insertion loss and isolation. The notation used here for insertion loss and isolation follows international practice. The symbol α is used to denote "attenuation"; numerical subscripts denote the sense. Thus α_{1-2} is the attenuation suffered by energy passing through the device from port *1* to port *2*. The order of the numbers in the subscript, in giving direction also defines the quantity: thus α_{1-2} is insertion loss, whereas α_{2-1} would be isolation.

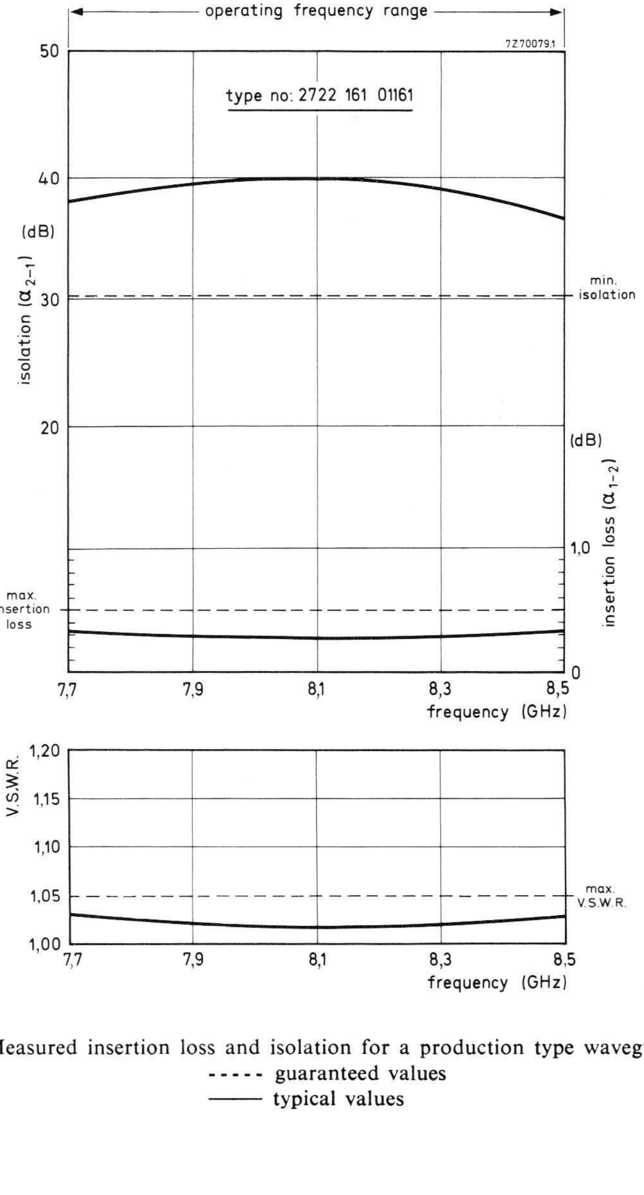

Fig. 16*b* Measured insertion loss and isolation for a production type waveguide isolator.
- - - - - guaranteed values
——— typical values

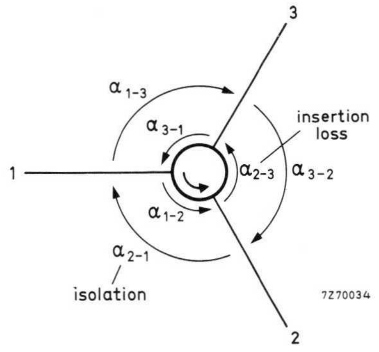

(a)

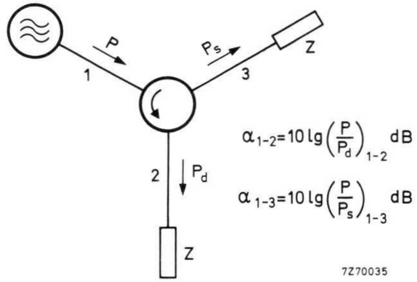

(b)

Fig. 17 At (*a*) the various insertion losses and isolations associated with a circulator are given using the "α" notation, and at (*b*) the power levels encountered are related to the circulator attenuations.

3.2 Circulators

In the case of a circulator, the insertion loss and isolation of each individual branch must be considered. These characteristics must also be measured with the device ports provided with matched terminations. The various attenuations are shown in Fig. 17, where the α-notation is extended to a three-port device.

A circulator cannot be considered in isolation! Reflection of energy from the other circuit elements to which it is connected will have a profound effect on the isolation realized in practice. Thus, assuming that ports *2* and *3* are not terminated, and a signal is injected by way of port *1*, as in Fig. 18, then, neglecting insertion loss, a signal level of $r_1{}^2 r_2{}^2 P$ will be reflected back to port *1* after the signal has traversed the circulator three times. (This situation is analysed in detail in the Appendix.)

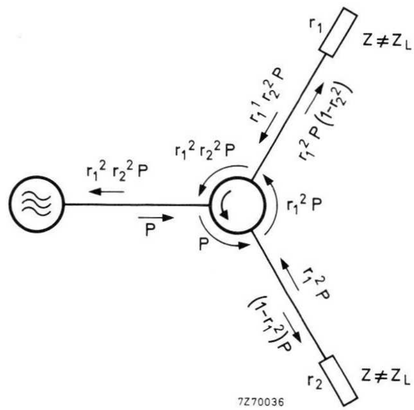

Fig. 18 When a circulator is not correctly terminated, power will be reflected and circulated several times.

4 Applications

Application of isolators and circulators will be considered for convenience under four main headings: decoupling and reflection suppression, signal separation, signal combining, and, finally, phase-shifting and modulation.

4.1 Decoupling and reflection suppression

When, at high frequencies, one device or module is used to supply power to a second, such as might be the case with two amplifiers in cascade, power reflection is an ever-present problem. Such reflection can be caused by mismatch or imperfect tuning, and can give rise to power changes, amplitude variations and non-linearities, and hence to a deterioration of signal quality. Constant loading of the signal source may be achieved by including an isolator in its output connection as in Fig. 19; reflections from the load will then be absorbed by the isolator to an extent which depends upon its isolation.

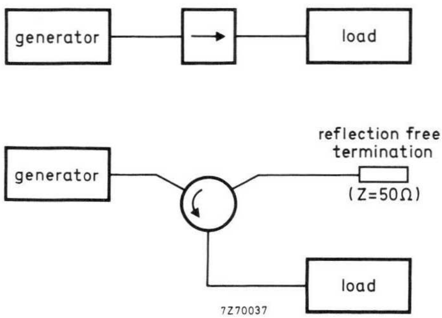

Fig. 19 The basic function of an isolator: decoupling a signal source from its load. Where high powers are involved, the use of a circulator permits the energy to be dissipated in an external termination.

Isolators for use at high power levels usually consist of a terminated circulator, the absorbed power being dissipated externally to the circulator, in the load forming the termination. At lower frequencies, less than about 2 GHz, where waveguides are not normally used, all isolators are in fact circulators with a matched termination on the third port. Waveguide isolators of the type described in this book are for use at higher frequencies and for handling power levels up to about 10 W, or for absorbing total reflected powers of about 3 W. Now some specific examples will be examined.

Where the input of a power amplifier is closely coupled to the output of a pre-amplifier, and either can react to changes in the other, sufficient isolation must be introduced between them to ensure proper decoupling. Here, isolation is the more important requirement.

Fig. 20 Interstage decoupling using an isolator: either stage may be tuned without the other being affected.

Fig. 20 shows an example of interstage decoupling. With the isolator in circuit, each stage may be tuned without the other being affected. Similar applications are illustrated in Figs 21 and 22, both involving decoupling an output stage from the aerial it feeds. In Fig. 21, the isolator not only prevents feedback from the aerial to the output stage, but also serves to protect the output stage itself in the event of the aerial being damaged or frozen over. In the application of Fig. 22, besides offering the foregoing advantages, the isolator also suppresses the multiple reflections caused by mismatch between an aerial and a long feeder.

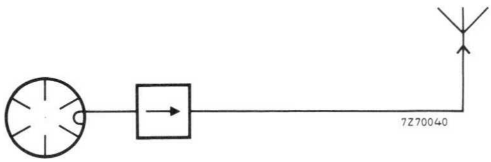

Fig. 21 Here an isolator is used to decouple a transmitter from its aerial.

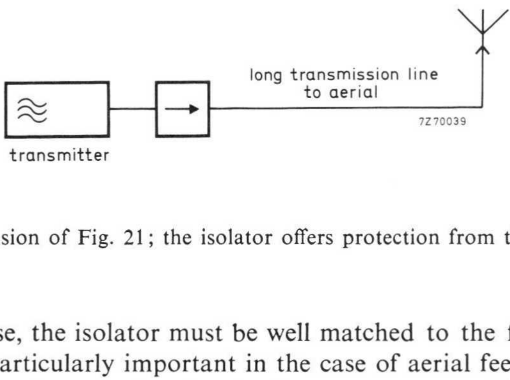

Fig. 22 An extension of Fig. 21; the isolator offers protection from the "long-line" effect.

For this purpose, the isolator must be well matched to the feeder. The "long line" effect is particularly important in the case of aerial feeders in communications systems, since ringing due to the reflections would result in a poor signal-to-noise ratio.

Similar advantages are to be obtained from the inclusion of isolators in test equipment, such as signal generators. Accuracy can often be improved in a measurement situation by decoupling the various equipments by means of isolators. In order to obtain maximum benefit from this technique, isolators offering high isolation should be connected immediately adjacent to the equipments concerned, see Fig. 23.

The inclusion of an isolator in the output circuit of a signal source, Fig. 24, allows the source impedance to be well defined.

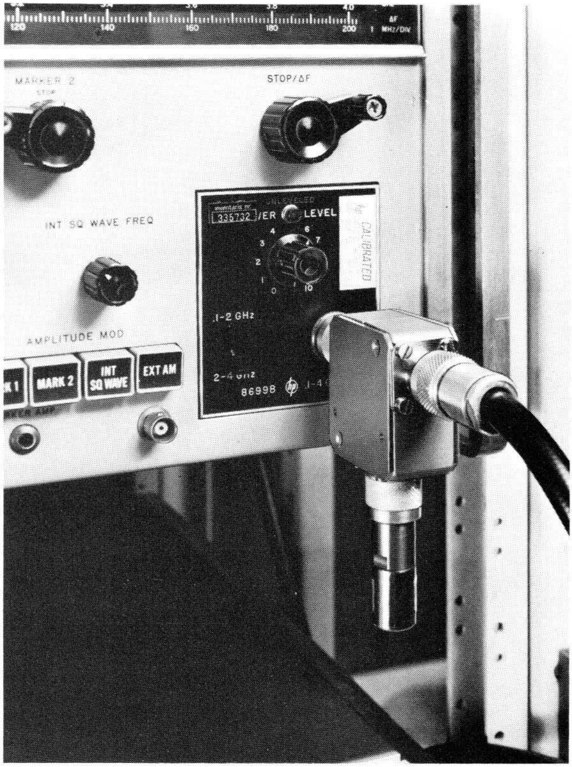

731204-05-02

Fig. 23 An example of the use of an isolator (isolator-connected circulator) in a measurement facility. An isolator should always be sited close to the equipment with which it is associated.

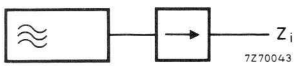

7Z70043

Fig. 24 Because the isolator is included, the generator always "sees" a constant load impedance. (See also the frontispiece.)

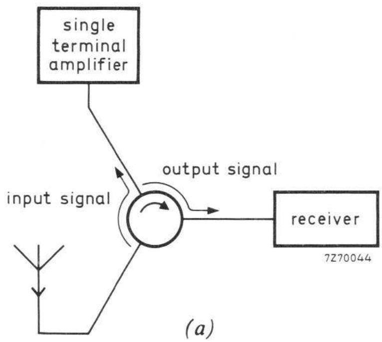

(a)

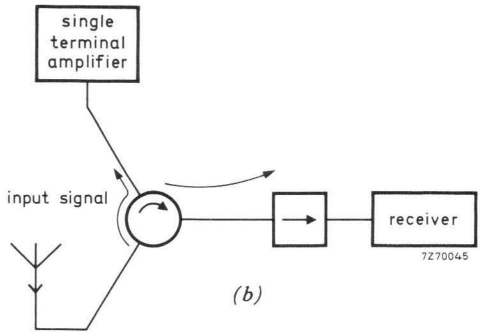

(b)

Fig. 25 A single-terminal amplifier, such as a parametric amplifier, requires a circulator to separate the incoming and amplified signals (*a*). Including an isolator (*b*) between the circulator and the receiver or following amplifier greatly improves the isolation between input and output and thus the maximum stable stage gain which can be employed.

4.2 Directional signal separation and switching

In those types of amplifier where the input and output signals traverse the same path (such as the parametric amplifier, tunnel diode amplifier, Gunn or IMPATT diode amplifier) the input and output can be separated by means of a circulator. Such an arrangement is shown in Fig. 25*a*, where a single-port amplifier is connected between an aerial and a receiver, and a circulator used to direct the incoming and amplified signals correctly. Both isolation and insertion loss are important in this application, particularly where a weak signal is to be received. Insertion loss should be low so that most of the signal in the aerial reaches the amplifier, and isolation must be high if regeneration and instability in the amplifier are to be prevented. A further refinement of the circuit is shown in Fig. 25*b* where an isolator is included between the circulator and the receiver, improving matching and the isolation achieved with the circulator. A similar arrangement can be used to feed trigger pulses to an oscillator or magnetron.

Similar considerations apply in the case of a transceiver operating on a single aerial, Fig. 26. Here, a circulator is used to separate the transmitted and received signals. This principle is employed in Doppler and pulsed radar sets, and in f.m. radio links. In a pulsed radar installation it is usual to incorporate further protection between circulator and receiver to protect the latter against the effects of limited isolation and power reflected back from the transmitter.

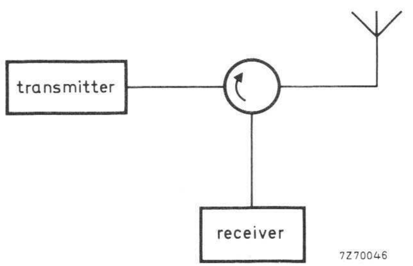

Fig. 26 Here a circulator permits a transmitter and receiver to share an aerial.

4.3 Signal combination: frequency-selective switches

Circulators are used to combine signals of differing frequency for radiation by a common aerial. A common example is the t.v. transmitter, the arrangement of which is shown in Fig. 27. The sound signal travels through the isolator to the circulator, is reflected by the filter and returns to the circulator whence it is directed to the aerial. Between filter and aerial both sound and vision signals traverse the same path. A steep-sided response characteristic is necessary in the filter since the sound carrier is only some 0,5 MHz from the edge of the video sideband. This method of signal combination introduces neither group delay nor non-linearity distortion.

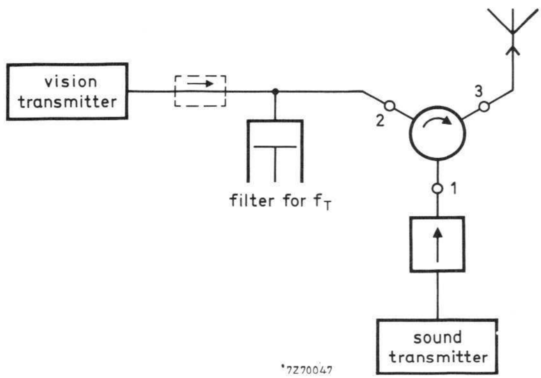

Fig. 27 Circulators are often employed to combine the sound and vision signals in a t.v. transmitter.

This technique may be extended to the combination of a large number of signals, as shown in Fig. 28. Here, each filter passes only the frequency band required by its associated transmitter, reflecting all others. The filter selectivities determine the minimum practicable separation between signals.

In a cascade system, circulator insertion losses are of great importance. If the number of stages is large, and the insertion losses high, the output obtained to the aerial from the most remote transmitter will be excessively attenuated. Furthermore, since the last circulator in the chain passes all the power, it must be chosen to have a sufficient signal-handling capability. (Further discussion of power and t.v. signal combining will be found in Section 9.)

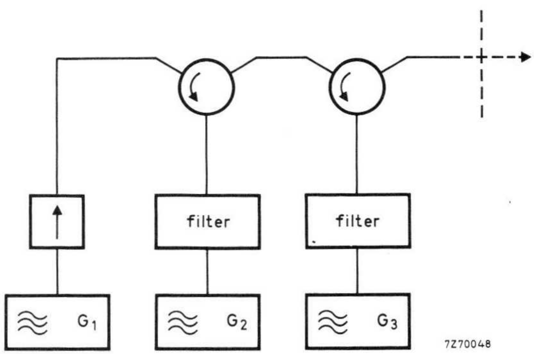

Fig. 28 Extension of the principle illustrated in Fig. 27. Here, several signals are combined together in one transmission path. The system may, of course, be extended indefinitely but a practical limit will be set by the insertion losses suffered by the signals which have to traverse many circulators.

The arrangement used for signal combining can be operated in reverse, as a receiver, enabling a mixture of input signals to be filtered and each directed to its appropriate amplifying or detector stages. Such a system is given in Fig. 29. The input is fed through a circulator to a bandpass filter, the accepted signal passes to the amplifier and the reflected signals return to the cirulator whence they are directed to an identical second stage.

The combining circuit of Fig. 28 and the separation circuit of Fig. 29 can be used together in a multi-channel tranceiver. The basic arrangement of such a system is given in Fig. 30. It should be noted that the order of remoteness of receiving channels is opposite to that of transmitting channels, so that each signal transverses the same number of circulators and suffers the same attenuation.

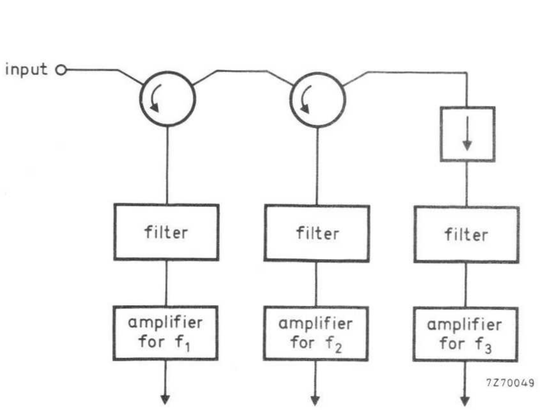

Fig. 29 Circuit arrangement complementing that of Fig. 28, allowing combinations of signals of differing frequency to be resolved.

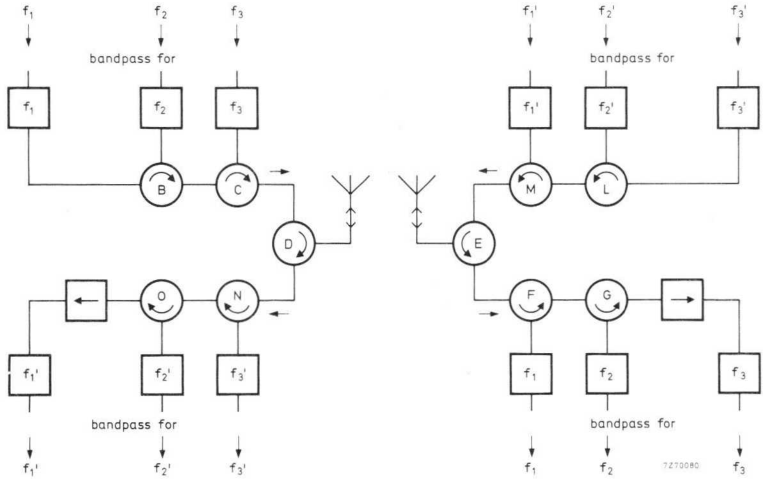

Fig. 30 The principles of signal combination and separation can be used together to design a frequency-multiplexed, multi-channel transceiver system. By reversing the order of combination and separation of signals, signal attenuation due to insertion losses can be made the same for all signals.

4.4 Circulators as modulators and variable attenuators

Just as a circulator with a matched load on its "free" port forms an isolator, so it is possible to obtain other circuit functions with other devices added. For example, a variable phase shifter can be constructed by adding a variable short circuit, as shown in Fig. 31, Such an arrangement can replace a telescopic or plunger type phase shifter, the reflection from the variable short circuit altering

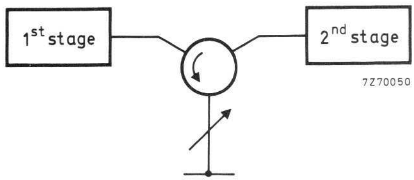

Fig. 31 Mechanically simpler than a telescopic phase shifter, this combination of a circulator and variable short circuit fulfils the same function.

the phase between the input and output signals of the circulator. In Fig. 32 the phase shifter is shown used to swing the beam of a dipole aerial array without the aerial itself being moved.

Both isolation and insertion loss are important parameters of circulators used in variable phase shifters. Insertion loss determines the attenuation of the circuit, while isolation sets the level of signals of the original phase reaching the aerial.

The variable phase shifter can be converted into a phase modulator by replacing the mechanically variable short circuit by an electronically variable one. One possible arrangement for such a device is shown in Fig. 33, where a varactor diode is used as a variable reactance. The diode is fed from a modulator, and the consequent variations in the phase of reflections cause phase modulation of the transmitter output. The circulator used must have a high reverse attenuation so that the transmitter output stage will not be affected by the modulator. If the aerial is not properly matched an isolator should be inserted, either between the circulator and the aerial, or, preferably, between the transmitter and the circulator where it will improve decoupling.

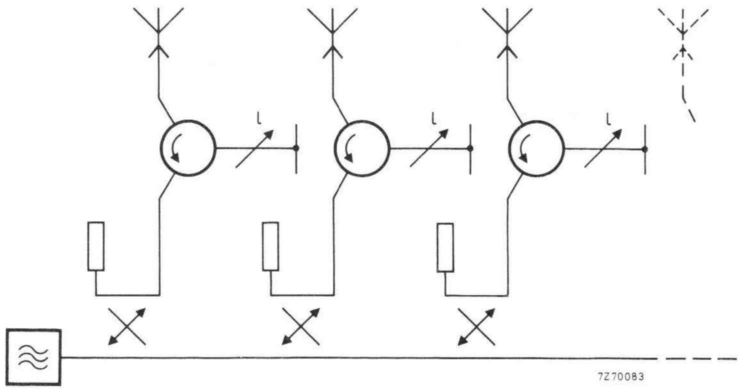

Fig. 32 Here the variable phase shifter is used to swing the beam of an aerial array.

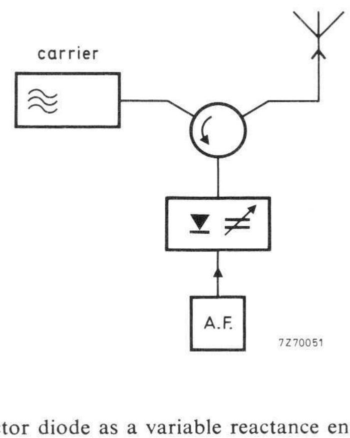

Fig. 33 The use of a varactor diode as a variable reactance enables the phase shifter to be used as a phase modulator.

Figure 34 shows a circulator used as part of a power control circuit. The arrangement comprises a fixed matched load and a variable short circuit; moving the short causes the amount of power dissipated in load to vary. Amplitude modulation can be achieved at low power levels by replacing the load and short circuit by a PIN diode.

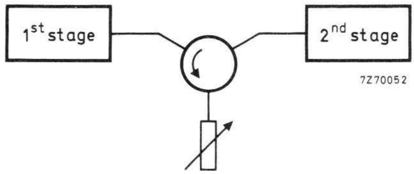

(a)

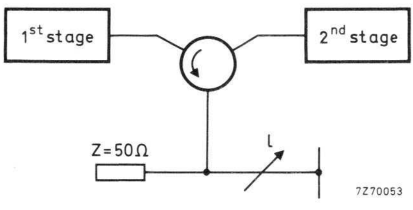

(b)

Fig. 34 In (*a*) a variable load connected to a circulator is used to alter or control the transmitted power level. In (*b*) the amount of power dissipated in the load is set by means of the associated variable short circuit.

The basic circuit of a pulse code modulator is shown in Fig. 35. Here, two circulators are used, terminated by modulator diodes and a $\lambda/4$ and $\lambda/8$ waveguide section. Circulators employed for pulse code modulation must have a particularly high isolation to prevent interaction between the various units in the system.

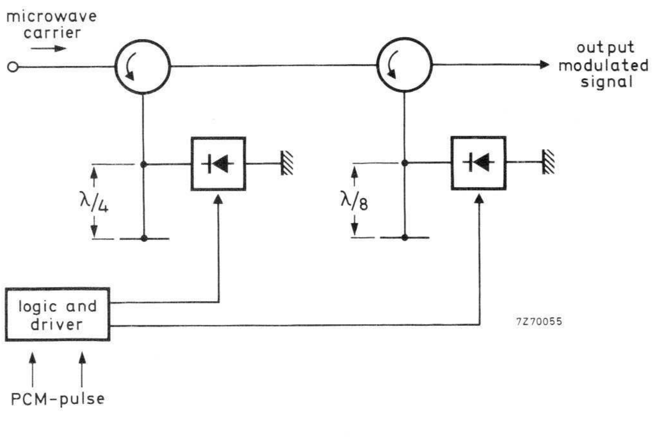

Fig. 35 Circulators used to form a pulse code modulator. Particularly high isolation is required in this application.

5 Multiport circulators

Circulators with more than three ports can, in principle, be formed by the interconnection of several 3-port circulators. Under ideal conditions – infinite isolation and negligible insertion loss – the port-to-port attenuations will be equal. In practice however these conditions are never met with, and in the configurations shown in Fig. 36 the insertion loss between ports *4* and *1* (α_{4-1}) or *2* and *3* (α_{2-3}) will be twice that between *1* and *2* (α_{1-2}) or *3* and *4* (α_{3-4}), whereas the isolation between *1* and *4* (α_{1-4}) or *3* and *2* (α_{3-2}) will be twice that between *2* and *1* (α_{2-1}) or *4* and *3* (α_{4-3}). It is thus possible to increase isolation at the expense of insertion loss, if this is considered acceptable.

True *4*-port circulators have lower insertion losses but smaller bandwidths than those formed with *3*-port circulators. The best known from of *4*-port circulator for high powers is the phase shifter circulator used in pulse radar equipement. As shown in Fig. 37, this consists of two non-reciprocal phase shifters and waveguide couplers ("magic T" and 3 dB hybrid). The coupling direction within the circulator can be reversed by switching the phase shifters.

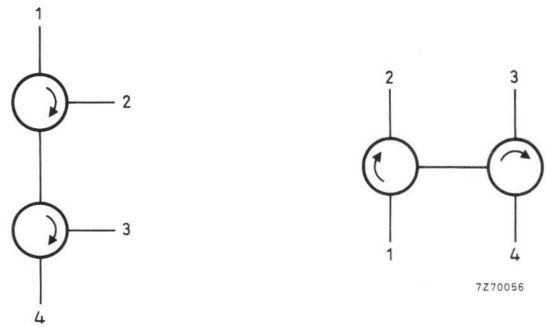

Fig. 36 Two interconnected three-port circulators simulating a four-port circulator.

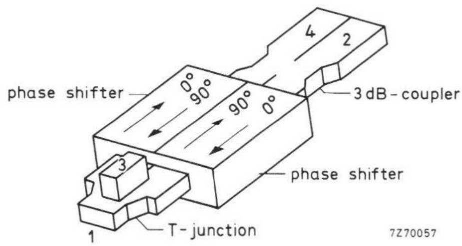

Fig. 37 A form of four-port circulator frequently encountered in pulse radar practice.

6 Switchable circulators and their applications

The coupling direction of a circulator is determined by the polarity of the magnetic field used to bias the ferrite. Reversing the direction of this field reverses the coupling direction of the circulator. Various means are employed to reverse the direction of the biasing field. Electromagnets may be used whose current is switched; alternatively, the polarity of permanent bias magnets could be reversed by means of a current pulse in a magnetizing winding.

The arrangement shown in Fig. 38 is typical of applications for reversible circulators. The several differently oriented aerials are fed sequentially by switching the coupling direction of the circulator. Figure 39 shows a reversible circulator used to select a small sector of the normal arc of scan of a radar aerial. This is useful in military applications where the scanning of only a small sector reduces the detectability of the installation.

The circuit of Fig. 40 is a development of Fig. 23. The isolators have been replaced by switchable circulators thus allowing the corresponding sources to be isolated. Output power from the isolated sources is dissipated in terminating resistors.

Complex microwave switching networks can be readily assembled from the simple, inexpensive switchable circulators now manufactured by the planar

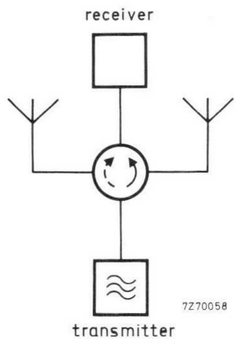

Fig. 38 Feeding two aerials of different orientation with a switchable circulator.

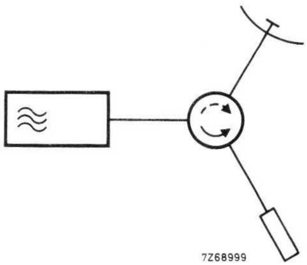

Fig. 39 Using a switchable circulator to restrict the arc of scan of a pulsed radar.

technique. Multiple branching and switching problems can easily be solved with these devices. When designing such networks, however, consideration must be given to whether or not, at low power levels, semiconductor or phase shift switches may not be more suitable.

If instead of switching the magnetic field from one polarity to the other, some provision is made for varying it, it becomes possible to construct narrow-band tunable circulators. The centre frequency of a tunable circulator of this type is capable of being varied over a wide range.

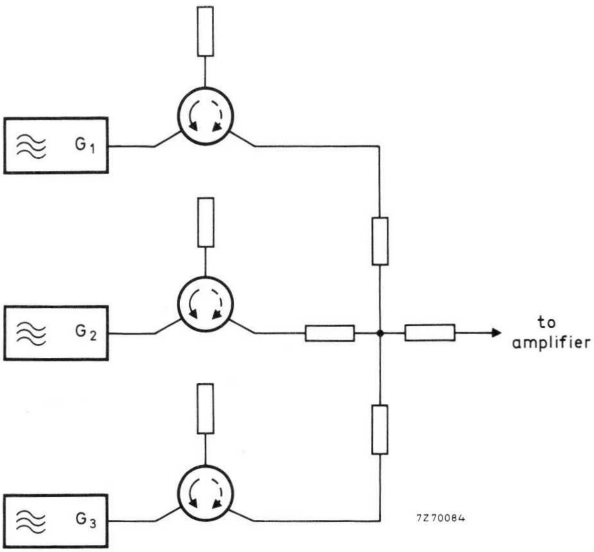

Fig. 40 Switchable circulators connected as isolators used to switch equipments in and out of a network.

7 Assessing input reflection

7.1 Defining reflection coefficient

Besides isolation and insertion loss, device properties which were defined in Section 3, another important parameter of all microwave components is reflection coefficient. This is the ratio, measured at one terminal, of the amplitude of the energy coming out to that going in:

$$\text{reflection coefficient, } r = \frac{\text{amplitude of outgoing wave}}{\text{amplitude of ingoing wave}}.$$

Reflection coefficient is related to v.s.w.r. (voltage standing wave ratio) by:

$$|r| = \frac{s-1}{s+1},$$

where s is the v.s.w.r. (see Fig. 41).

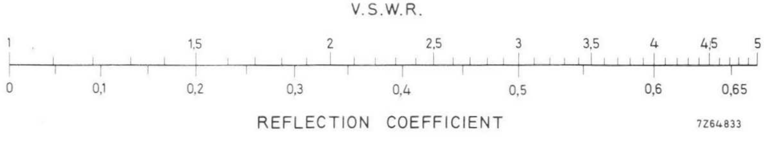

Fig. 41 Scale for converting reflection coefficient to v.s.w.r.

The reflection coefficient at one port of a circulator must be measured with the other ports correctly terminated, otherwise the measured value will be in error.

7.2 Reflection in isolator-connected circulators

Circulators provided with a load on the third port are used as isolators for decoupling purposes; see by way of example, Figs 19 and 20. In such cases, a maximum v.s.w.r. will be specified for the source, which is defined by the nature of the source itself. The relationship between v.s.w.r. and reflection coefficient was given in the preceding section.

The consequences of reflection will be discussed with reference to Fig. 42 which shows an isolator-connected circulator used to couple a generator to its load. The reflection coefficients associated with this duty are r_1 and r_L, which for the sake of simplicity are assumed to be of the same order of magnitude. The coefficient r_1 is the complex input reflection coefficient of the circulator appearing at the output if the other ports are provided with matched terminations. Also complex are the input and output voltages V_1 and V_2, whilst r_L is the input reflection coefficient of the load (an additional amplifier stage, for example).

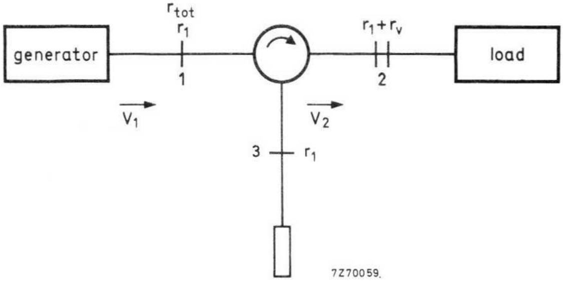

Fig. 42 Reflections associated with the use of an isolator-connected circulator.

The value of r_1 normally associated with a circulator is well less than unity so that the power lost by the reflected wave, $r_1 V_1$, at the input can generally be ignored. The amplitude, V_2, of the reflected waves at port *2* is

$$V_1 \sqrt{1 - |r_1|^2} \cdot \exp j\phi_1,$$

and has almost its original value (ϕ_1 is the phase shift between V_1 and V_2). Here the insertion loss is neglected. The voltage $(r_1 + r_L)V_2$ is reflected by the load and reaches port *3*, where it encounters a small reflection of coefficient r_1. A voltage $r_1(r_1 + r_L)V_2$ is reflected by the load and reaches port *1*, the input, and is added (depending on both the phase shift and the path taken) to the directly reflected voltage $r_1 V_1$, so that, in total, a voltage of

$$r_1 V_1 + r_1(r_L + r_1)(1 - |r_1|^2) V_1 \cdot \exp j\phi$$

is fed from the input to the source. Thus the total effective reflection coefficient, r_{tot}, becomes

$$r_{\text{tot}} = r_1 \{1 + (r_1 + r_L)(1 - |r_1|^2) \cdot \exp j\phi\}.$$

If it is assumed that the power loss at the input port can be neglected, and that the phase of the reflection from the load is at its most unfavourable, then the maximum r_{tot} is found from

$$r_{\text{tot}} = |r_1|\{1 + |r_1| + |r_L|\} \tag{1a}$$

If the load v.s.w.r. is significantly larger than the circulator v.s.w.r., Eq. (1*a*) may be simplified to

$$|r_{\text{tot}}| = |r_1|(1 + |r_L|). \tag{1b}$$

Now $|r_{\text{tot}}|$ will be chosen to be the maximum tolerable in the system (the maximum permitted v.s.w.r. for a magnetron for example), and since $|r_L|$ set sthe maximum reflection encountered from the load, $|r_1|$ can be calculated from

$$|r_1| = \sqrt{\left(\frac{1 + |r_L|}{2}\right)^2 + |r_{\text{tot}}|} - \frac{1 + |r_L|}{2}$$

or, with Eq. (1*b*):

$$|r_1| = \frac{|r_{\text{tot}}|}{1 + |r_L|}.$$

Complete specification of an isolator (isolator-connected circulator) requires that the necessary amount of isolation for a particular application be known. As with input reflection, isolation can be expressed in terms of the energy returned to the source. For a circulator with reflection-free terminations, the isolation between input and output may be expressed as

$$\alpha_{1-3} = 20 \log \frac{1}{|r_1|} \text{ (dB)}$$

so that input reflection can, to a certain extent, be taken as a measure of isolation.

Without going further into general network considerations, see Appendix, this can be explained as follows. Let a circulator be terminated at ports *2* and *3* by terminations of reflection coefficient r_1 and be driven in the reverse direction, as in Fig. 43. In these circumstances the amplitude of the wave at port *1* travelling

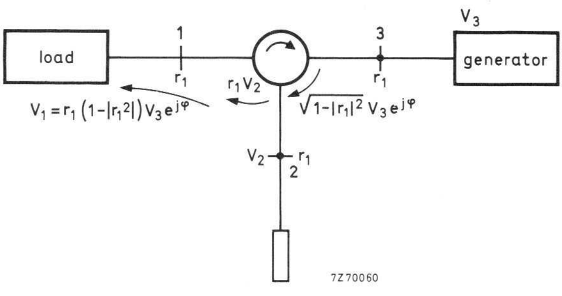

Fig. 43 Derivation of the value of isolation.

towards the load can be regarded as a measure of the isolation. The amplitude of this wave is

$$r_1(1 - |r_1|^2) \cdot \exp j\phi V_3$$

or since $|r_1|$ is much less than unity:

$$V_1 = r_1 V_3 \cdot \exp j\phi.$$

Now the isolation is given by $|V_1|/|V_3|$, so from the expression given above for V_1, the following useful expression can be derived:

$$\alpha_{1-3} = 20 \log \frac{|V_1|}{|V_2|} = 20 \log |r_1| .$$

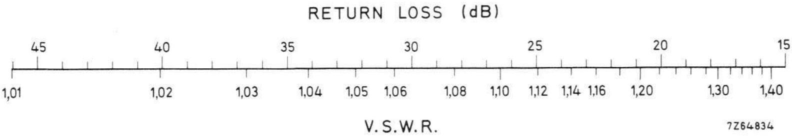

It is now possible to write down the requirements for an isolator-connected circulator used to connect a source to its load.

The minimum permissible isolation is

$$\alpha_{1-3\,\min} = 20 \log \left\{ \left(\frac{s_m - 1}{s_m + 1} + \frac{s_L{}^2}{(s_L + 1)^2} \right)^{\frac{1}{2}} - \frac{s_L}{s_L + 1} \right\} \tag{2}$$

or, if r_1 is negligible compared to r_L:

$$\alpha_{1-3\,\min} = 20 \left(\log \frac{s_m - 1}{s_m + 1} - \log \frac{2 s_L}{1 + s_L} \right) \tag{3}$$

where s_m is the maximum permissible v.s.w.r.

A nomogram calculated from this relationship, which saves a considerable amount of labour, appears as Fig. 44.

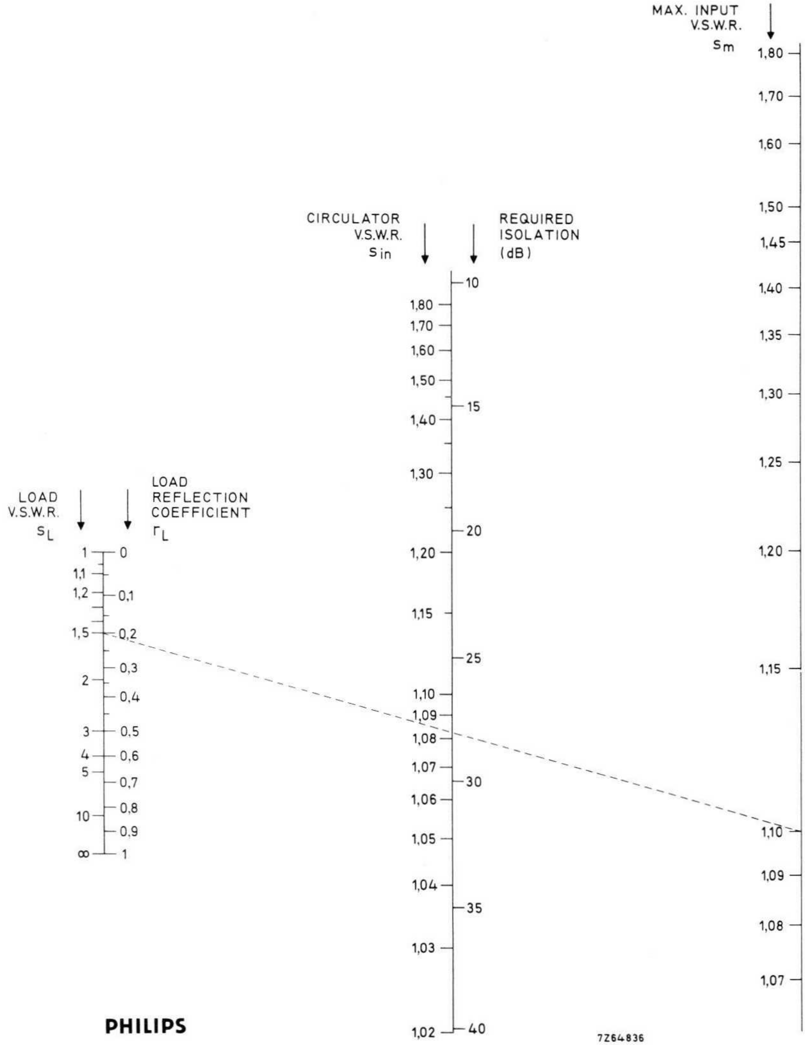

Fig. 44 Nomogram showing the approximate relationship between load and input v.s.w.r., and circulator input v.s.w.r. and isolation. The expansion of the various scales accurately reflects the importance of the various quantities in terms of the final result obtained.
The example shows that a circulator required to present an input v.s.w.r. of 1,10 when provided with a load of v.s.w.r. 1,5 should have a v.s.w.r. of 1,08. This result should be checked with the aid of Fig. 46

Example

Let s_L, the load v.s.w.r., be 1,5, and let the maximum permissible v.s.w.r. to be presented to the source, s_m, be 1,10. The minimum isolation of the circulator or isolator to be used can then be calculated from the equations given above. The approximate expression, Eq. (3) yields a value of 28,03 dB, whereas Eq. (2) gives 28,29 dB. This situation is that given on the nomogram above.

8 Circulators in circuit

As already explained in Section 3.2, the performance of a circulator may be defined in terms of input reflection, isolation, and insertion loss. These quantities and their temperature dependence are, in practice, heavily influenced by the circuit elements connected to the ports of the circulator. In the following Sections the influence of external circuitry on the performance of a *3*-port circulator will be examined in more detail.

Those circulator characteristics which are susceptible to experimental determination will, of course, be of particular interest to the user. Among these characteristics are permissible ambient temperature, maximum continuous and peak loads, and corrosion resistance; these are discussed in the following sections and in published circulator data.

8.1 Transformation matrix for a lossless, cyclic symmetrical, 3-port circulator

The calculations given in this Section, included for the sake of completeness, might be omitted at the first reading.

The relationships between the input properties of lossless, cyclic symmetrical, *3*-port circulators may be clarified by considering a linear *3*-port circulator. In general a *3*-port circulator has the scattering matrix S, such that

$$\begin{pmatrix} b_1 \\ b_2 \\ b_3 \end{pmatrix} = \begin{pmatrix} S_{11} & S_{12} & S_{13} \\ S_{21} & S_{22} & S_{23} \\ S_{21} & S_{32} & S_{33} \end{pmatrix} \begin{pmatrix} a_1 \\ a_2 \\ a_3 \end{pmatrix}_{(b) = (S)(a)} \tag{4}$$

where a_ν represents the input waves, and b_ν the output waves. The only qualification in the expression is linearity, that is, the matrix elements $S_{\mu\nu}$ must be independent of the quantities a_1, a_2, a_3 and b_1, b_2, b_3. The elements of the scattering matrix have a definite meaning, input reflection, isolation and so forth. These will be discussed in Section 8.2.

The non-reciprocal nature of a multi-port circulator is reflected in the asymmetry of its scattering matrix:

$$\begin{pmatrix} S_{11} & S_{12} & S_{13} \\ S_{21} & S_{22} & S_{23} \\ S_{31} & S_{32} & S_{33} \end{pmatrix} \neq \begin{pmatrix} S_{11} & S_{21} & S_{31} \\ S_{12} & S_{22} & S_{32} \\ S_{13} & S_{23} & S_{33} \end{pmatrix}_{S \neq S^*.} \tag{5}$$

So that if $S_{12} \neq S_{21}$, $S_{13} \neq S_{31}$, $S_{23} \neq S_{32}$, the device is non-reciprocal. A circulator may be defined as lossless if the sum of the input powers equals the sum of the output powers. Expressed in the form of a matrix, this means that the product of the scattering matrix, S, with the transposed, conjugate complex scattering matrix S'^* equals the unity matrix E:

$$\begin{pmatrix} S_{11} & S_{12} & S_{13} \\ S_{21} & S_{22} & S_{23} \\ S_{31} & S_{32} & S_{33} \end{pmatrix} \cdot \begin{pmatrix} S_{11}^* & S_{21}^* & S_{31}^* \\ S_{12}^* & S_{22}^* & S_{32}^* \\ S_{13}^* & S_{23}^* & S_{33}^* \end{pmatrix} = \begin{pmatrix} 1 & 0 & 0 \\ 0 & 1 & 0 \\ 0 & 0 & 1 \end{pmatrix}_{S \cdot S'^* = E \cdot} \tag{6}$$

A multi-port circulator has cyclic symmetry when its parameters remain unchanged if the inputs undergo cyclic switching. This can appear in the scattering matrix, in that each line must follow from the preceding one in a similar cyclic manner. In this case the components of each line shift one position to the right:

$$\begin{pmatrix} S_{11} & S_{12} & S_{13} \\ S_{21} & S_{22} & S_{23} \\ S_{31} & S_{32} & S_{33} \end{pmatrix} = \begin{pmatrix} S_{11} & S_{12} & S_{13} \\ S_{13} & S_{11} & S_{12} \\ S_{12} & S_{13} & S_{11} \end{pmatrix} = \begin{pmatrix} S_{22} & S_{23} & S_{21} \\ S_{21} & S_{22} & S_{23} \\ S_{23} & S_{21} & S_{22} \end{pmatrix} = \begin{pmatrix} S_{33} & S_{31} & S_{32} \\ S_{32} & S_{33} & S_{31} \\ S_{31} & S_{32} & S_{33} \end{pmatrix}. \tag{7}$$

In the case of cyclic symmetry, that is if

$$\begin{aligned} S_{11} &= S_{22} = S_{33} = S_1, \\ S_{12} &= S_{23} = S_{31} = S_2, \\ S_{13} &= S_{21} = S_{32} = S_3, \end{aligned}$$

but $S_2 \neq S_3$ (which is the condition for non-reciprocity), then the device under consideration is non-reciprocal and cyclically symmetrical in addition to being a three-port. This can be expressed by a more simple scattering matrix:

$$S = \begin{pmatrix} S_1 & S_2 & S_3 \\ S_3 & S_1 & S_2 \\ S_2 & S_3 & S_1 \end{pmatrix}. \tag{8}$$

According to Butterweck [4], the unity requirement results in the following expressions. From Eq. (6):

$$\begin{aligned} 1 &= S_1^* S_1 + S_2^* S_2 + S_3^* S_3 = |S_1|^2 + |S_2|^2 + |S_3|^2 \\ 0 &= S_1^* S_2 + S_3^* S_1 + S_2^* S_3 \\ 0 &= S_1^* S_3 + S_3^* S_2 + S_2^* S_1. \end{aligned}$$

It follows from these relationships, that not all combinations of values for S_1,

S_2 and S_3 are possible. The permissible combination of $|S_2|$ and $|S_3|$ values is shown graphically in the $|S_2|$, $|S_3|$ plane of a curvilinear triangle (Fig. 45) bounded by elliptical sectors.

$$\begin{aligned}
&|S_2|^2 + |S_2|\,|S_3| + |S_3|^2 - |S_2| - |S_3| = 0 \\
&(\text{Midpoint } |S_2| = \tfrac{1}{3};\ |S_3| = \tfrac{1}{3};\ \text{long axis } -45^\circ), \\
&|S_2|^2 - |S_2|\,|S_3| + |S_3|^2 + |S_2| - |S_3| = 0 \\
&(\text{Midpoint } |S_2| = -\tfrac{1}{3};\ |S_3| = \tfrac{1}{3};\ \text{long axis } +45^\circ), \\
&|S_2|^2 - |S_2|\,|S_3| + |S_3|^2 - |S_2| + |S_3| = 0 \\
&(\text{Midpoint } |S_2| = \tfrac{1}{3};\ |S_3| = -\tfrac{1}{3};\ \text{long axis } +45^\circ).
\end{aligned} \tag{9}$$

The possible values for $|S_2|$, $|S_3|$ are located within the shaded area. (Large half axis $\sqrt{2/3}$, small half axis $\sqrt{2/3}$.) Similar equations can also be set up for the $|S_1|$, $|S_3|$ and the $|S_1|$, $|S_2|$ planes.

If the sense of rotation of the circulator is taken as 1-2-3-1, and $|S_2| \approx 1$ for the insertion loss, $|S_3| \leqslant 1$ for the isolation, it is found via row development that the possible addition of the values of the matrix elements is located in the vicinity of the right-hand angle of the curvilinear triangle.

$$\begin{aligned}
1 - |S_3|^2 - |S_3|^3 - 2|S_3|^4 \ldots \leqq |S_2| \leqq 1 - |S_3|^2 + \\
+ |S_3|^3 - 2|S_3|^4 \ldots, \\
1 - |S_1|^2 - |S_1|^3 - 2|S_1|^4 \ldots \leqq |S_2| \leqq 1 - |S_1|^2 + \\
+ |S_1|^3 - 2|S_1|^4 \ldots .
\end{aligned} \tag{10a}$$

The relationships between $|S_2|$ and $|S_1|$, $|S_3|$ are only needed for measuring the input reflection and the isolation. The corresponding expression for a graph in the $|S_1|$, $|S_3|$ plane shows that the following conditions obtain in the vicinity of the origin:

$$\begin{aligned}
|S_3| - |S_3|^2 + |S_3|^3 - 2|S_3|^4 \ldots \leqq |S_1| \leqq |S_3| + |S_3|^2 + \\
+ |S_3|^3 + 2|S_3|^4 \ldots, \\
|S_1| - |S_1|^2 + |S_1|^3 - 2|S_1|^4 \ldots \leqq |S_3| \leqq |S_1| + |S_1|^2 + \\
+ |S_1|^3 + 2|S_1|^4 \ldots .
\end{aligned} \tag{10b}$$

Fig. 46 is a development of Fig. 45, allowing the actual values to be assigned to the attainable combinations of input v.s.w.r. and isolation.

A further discussion of the properties of the lossy circulator will be found in the Appendix.

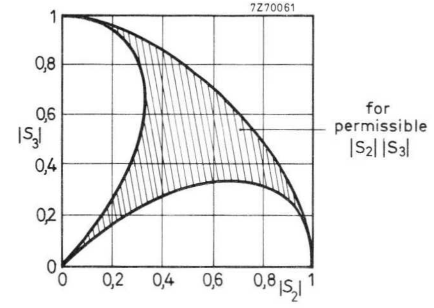

Fig. 45 Permissible combinations of $|S_2|$ and $|S_3|$.

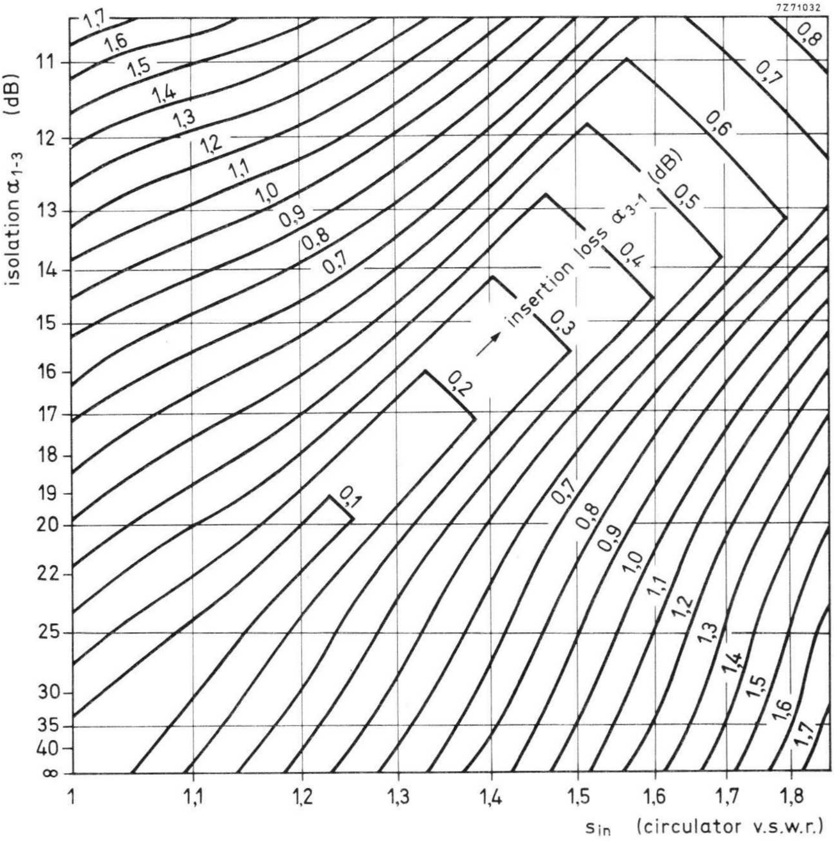

Fig. 46 One corner of the diagram of Fig. 45 expanded to give permissible combinations of input v.s.w.r. and isolation.

8.2 Practical results of the relationships between circulator characteristics

The theoretical relationships between input reflection, insertion loss and isolation, are discussed in some depth in the Appendix. In this section methods and results of measurement of these characteristics will be given by way of illustration.

Some of the measuring equipment used in the development and characterization of isolators and circulators is shown below. The principal measuring instrument is a (Hewlett-Packard) network analyser, which is supplemented by a Phase-Magnitude Display Module (type 8412). This instrument displays reflection coefficient on a logarithmic scale.

Examples of measured performance are illustrated by means of oscillograms. The curves start at the lower frequency (470 MHz) of the selected test sample, on the left, and end at the right at the upper frequency (600 MHz), Figs 47 to 57.

In all the figures, the upper curve is the 0 dB line which serves as a reference. This is of particular importance when evaluating empirical instrument settings (0,25 dB/div), for at higher frequencies the 0 dB line sometimes cannot be made to coincide with a grid line.

The bottom curve is the actual measured curve. Since with circulators the input reflection, isolation, and insertion loss are numerically less than one, and the logarithmic scale includes negative values, the measured curves are below the 0 dB line: as close to it as possible for the required low insertion loss, and as far below it as possible for the required high isolation.

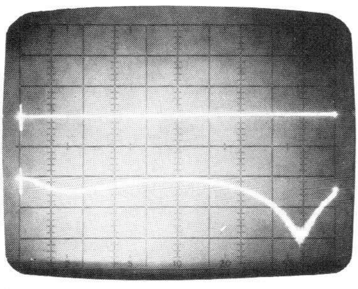

Fig. 47 Input reflection $|b_1/a_1|$ measured at port *1* of a 50 Ω circulator with ports *2* and *3* terminated by 50 Ω loads.

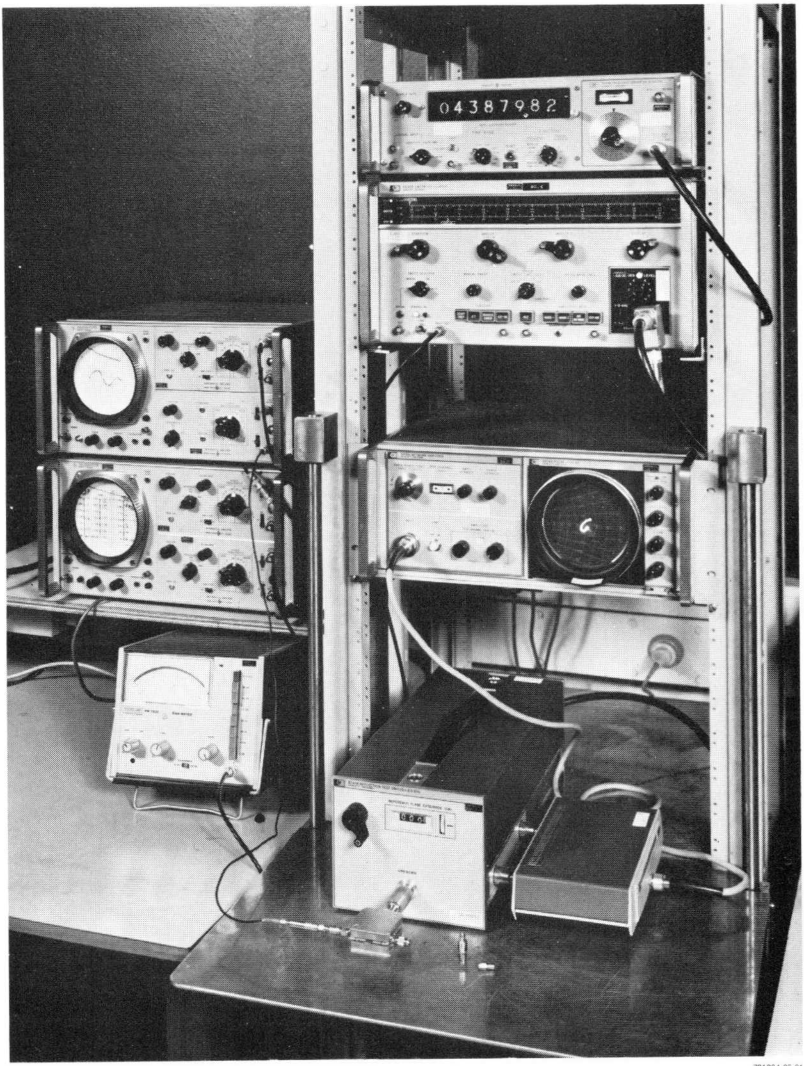

731204-05-01

A test facility used for measuring circulator performance.

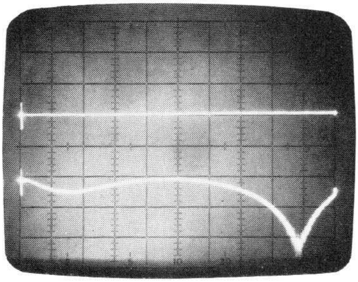

Fig. 48 Input reflection $|b_1/a_1|$ measured at port *1* of a 50 Ω circulator; here port *2* is terminated by a 60 Ω load and port *3* by a 50 Ω load. Terminations are connected directly on the ports. Compared with Fig. 47, reflection is only significantly affected in the upper part of the frequency range, at a reflection level of 30 to 40 dB.

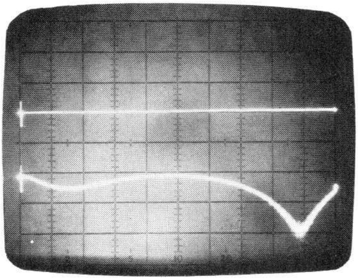

Fig. 49 Input reflection $|b_1/a_1|$ measured at port *1* of a 50 Ω circulator (10 dB/div.). Port *2* is terminated directly at the port by a 60 Ω load. There are no significant differences as compared with Fig. 47.

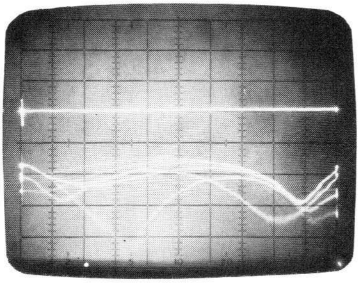

Fig. 50. Input reflection $|b_1/a_1|$ measured at port *1* of a 50 Ω circulator (10 dB/div.). Here, port *2* is terminated by a movable short-circuit and port *3* by a 50 Ω load. Reflection is displayed at six short-circuit positions. As compared with Fig. 47, a maximum increase of reflection coefficient of 6 dB is observed, while at some positions of the short-circuit, reflection coefficient can decrease.

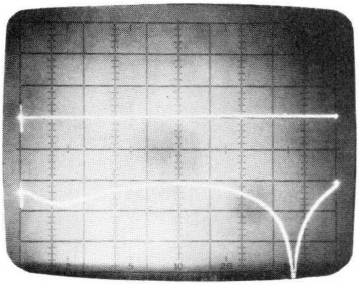

Fig. 51 Isolation $|b_3/a_1|$ (α_{1-3}) measured between ports *3* and *1* of a 50 Ω circulator (10 dB/div.). Port *2* is terminated by a 50 Ω load. The isolation characteristic has a similar structure to the curve of Fig. 47, but there are distinct differences.

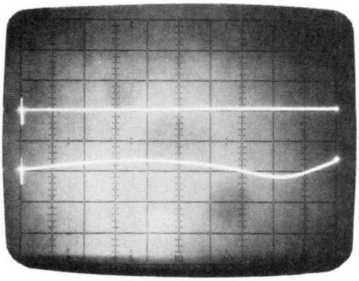

Fig. 52 Isolation $|b_3/a_1|$ measured between ports *3* and *1* of a 50 Ω circulator (10 dB/div.). Port *2* is terminated directly at the port with a 60 Ω load. As compared with Fig. 51, isolation has decreased considerably.

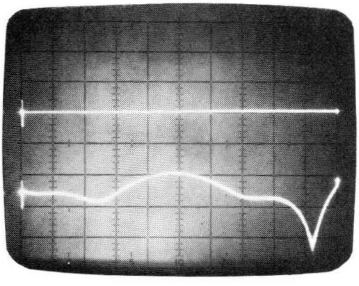

Fig. 53 Isolation $|b_3/a_1|$ measured between ports *3* and *1* of a 50 Ω circulator (10 dB/div.). For these measurements, port *2* was ter minated with a 60 Ω resistor connected through 1,5 m of RG-98U co-axial cable. The characteristic seems to be composed of the curve of Fig. 51, but with a wave superimposed on it. The isolation is reduced in the centre portion of the curve.

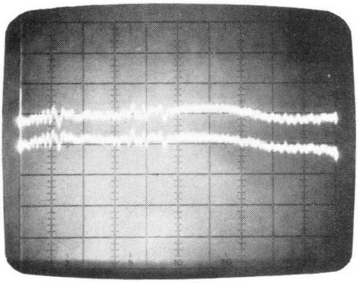

Fig. 54 Insertion loss $|b_2/a_1|$ (α_{1-2}) measured between ports *1* and *2* of a 50 Ω circulator, port *3* being terminated with a 50 Ω load. Owing to the high sensitivity (0,25 dB/div.) needed, equipment noise and non-linearity effect are visible both in the displayed characteristic curve and in the reference line. After averaging to eliminate the noise "grass", the measured isolation is obtained from the line separation.

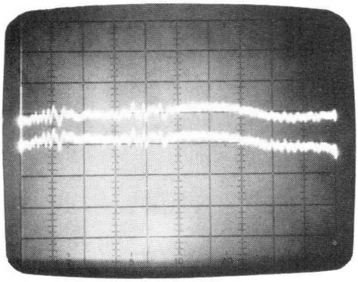

Fig. 55 Insertion loss $|b_2/a_1|$ measured between ports *1* and *2* of a 50 Ω circulator (0,25 dB div.). Here, port *3* is terminated with a 60 Ω load directly at the port and a further 60 Ω load connected by a 1,5 m length of co-axial cable type RG-98U. There are no differences between this curve and that of Fig. 54.

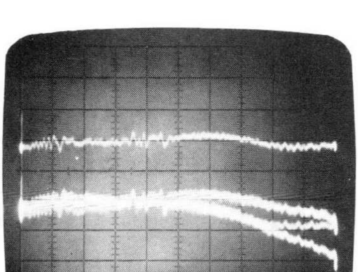

Fig. 56 Isolation $|b_3/a_1|$ (α_{3-1}) measured between ports *3* and *1* of a 50 Ω circulator (0,25 dB/div.). For these measurements, port *2* was terminated with a 4-position short-circuit. Power is transferred from port *2* to port *3*. Owing to internal reflections and multiple path transmission, only the order of magnitude of the insertion loss can be determined from this type of measurement which is thus not recommended as a measurement technique.

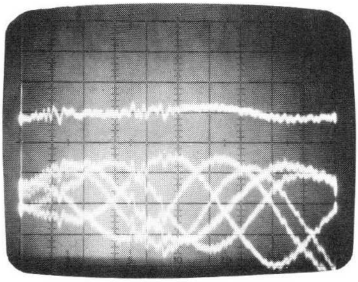

Fig. 57 Input reflection $|b_1/a_1|$ measured at port *1* of a 50 Ω circulator. Port *2* was terminated with a short circuit, and port *3* with a 5-position moveable short-circuit. Because internal reflections and multiple path transmissions occur, the triple insertion loss can only be approximately determined by averaging the curve shapes; this is thus not a recommended procedure.

8.3 General directions for circulator measurements

When measuring the input reflection and insertion losses of a circulator, the general rules of microwave measurement must be observed. The following are some of the most important:

- The generator must match the characteristic impedance of the connecting line (if required, an isolator must be inserted) to avoid the power changing due to the various terminations.
- Directional couplers have a directional effect on the measured value.
- Terminating resistors must not only be as reflection-free as possible, they must also have the same connectors as the circulator since adapters will give rise to additional reflections.
- Detectors should be reflection-free and, if necessary, be made to match by means of matching attenuators (e.g. 10 dB) or isolators of sufficiently low reflection coefficient.
- The sensitivity of the indicating instrument (tube voltmeter, oscilloscope) must be adapted to the detector sensitivity. With crystal detectors the d.c. voltage must be kept below 10 mV if the device is to work within its square-law region.

9 Power limits

The power limits of circulators and isolators are defined by three factors:

- temperature,
- internal arcing,
- non-linear effects.

Like all components, circulators are not entirely lossless, and so a certain amount of the h.f. energy is dissipated as heat. The temperature inside the circulator should not exceed a certain limit, as otherwise both the microwave ferrite and the magnet will show an unacceptable change in behaviour. If, for instance, the input power is 1 kW, and the insertion loss 0,3 dB (6 %), the total amount of power dissipated as heat will be 60 W. This causes a rise in the component temperature which must be added to the ambient temperature to arrive at the actual working temperature, the limit of which depends on the design.

When a circulator carrying r.f. power is not provided with properly matched terminations several difficulties may arise. For example, if one port of the circulator in the above illustration "sees" a termination which reflects all the energy incident upon it, then, since this power will traverse the circulator twice, the power dissipated in the ferrite will be doubled to 120 W. Given that the maximum working temperature of the circulator is 100 °C, and assuming that the 120 W dissipation causes a temperature increase of 60 °C, then the ambient temperature must be kept below 40 °C. Normally only the last figure, the ambient temperature, will be published in the manufacturer's data, ensuring that the circulator will remain within its temperature ratings under all conditions.

A second power limit is set by internal arcing. This may occur in regions of excessive field intensity, causing tracking across the ferrite and sparking between internal conductive parts of the circulator. With regard to the latter, it should be noted that wide-band circulators are fitted with thin ferrite discs, and the gap between the conductors placed either side of them is fairly small. Operation with high peak electric field intensities would require relatively large air gaps between these conductors. It will be apparent that the designer of a circulator is faced with conflicting requirements. During the development of a circulator, where emphasis is to be laid on wide-band operation, secondary measures are taken to reduce the likelihood of arcing. These include the rounding off of sharp corners.

The third effect which can dictate an upper power limit is the occurrence of electron spin waves in the ferrite of what are known as under-resonance circulators (see Section 2.2). The correct operation of a circulator requires that the sum total of h.f. magnetic field components be small compared to the magnetic biasing field. At very high power levels this may not be the case, and highly undesirable effects might occur, such as a non-linear behaviour of the circulator and a strong increase of the losses due to the generation of coupled resonances, so-called spin waves.

When developing ferrites for circulators, measures are taken to suppress these effects: by making ferrites with the finest possible crystal structure, and by introducing atoms with special characteristics into the crystal lattice. The discontinuous structures thus obtained largely suppress the occurrence of spin waves at h.f. power levels. Unfortunately, this latter method also disturbs the precessional motion of the electron spins, thereby introducing further insertion losses.

9.1 Average and peak powers, different signals

When a circulator is used to combine several signals (Figs 27 to 30), the average of the powers P_1, P_2 of the individual signals

$$P_1 + P_2 \ldots = \bar{P} \tag{14}$$

and the peak power, e.g. the power at maximum float

$$(\sqrt{P_1} + \sqrt{P_2} + \ldots)^2 = P_M \tag{15}$$

must both be taken into account.

Fig. 27 shows vision and sound signal combination. As the sound power P_s passes twice through the circulator, the average power, for $P_s = 0{,}2\,P_{sync}$ for instance, is

$$\bar{P} \approx 0{,}77\,P_{sync} + P_s + P_s = 1{,}17\,P_{sync},$$

where P_{sync} is the power in the sync pulse.

Under worst-case conditions the peak power produced when all required voltages are summed amounts to

$$P_M = (\sqrt{P_{sync}} + 2\sqrt{P_s})^2 = P_{sync}(1 + 2\sqrt{0,2})^2 = 3,6\,P_{sync}.$$

Where the same signal circulates several times, the peak voltage produced in the circulator depends on the phase angle of the reflected signal. Again, the filter-to-circulator distance is of great importance.

9.2 Average and peak powers at multiple circulation of one signal

Unless otherwise stated, the maximum powers quoted in the technical data are the highest powers a circulator can stand if one port is mismatched (v.s.w.r., $s = 2$ for all phase angles) whilst the next port is terminated with $s > 1,2$ (Fig. 58). With increased mismatch the average power flowing through the circulator is expressed as:

$$\bar{P}(|r_2|, |r_3|) = \bar{P}_1 (1 + |r_2|^2 + |r_3|^2 |r_2|^2). \tag{16}$$

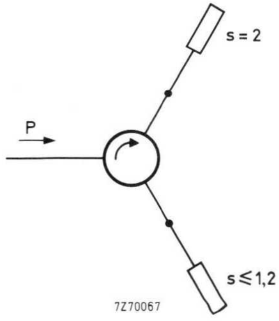

Fig. 58 Permissible v.s.w.r. values for maximum power.

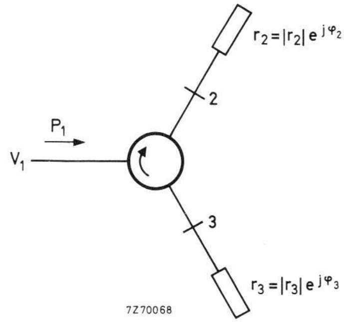

Fig. 59 Symbols for multiple circulation.

For determining the maximum power it is useful to start from the total voltage V_{tot} across the circulator (see Fig. 59).

In summing the partial voltages, the circulator can be subjected to high local peak power values which may even give rise to breakdown (flashover). Using the complex reflection factors $r_2 = |r_2| \cdot \exp j\phi_2$ and $r_3 = |r_3| \cdot \exp j\phi_3$, we arrive at

$$V_{tot} = V_1 + V_1 r_2 \cdot \exp j\phi'_2 + V_1 r_3 \cdot \exp j\phi'_3 r_2 \cdot \exp j\phi'_2.$$

The phase angles ϕ'_2 and ϕ'_3 result from the paths through the conductors. The power is expressed as:

$$P \approx V_{tot} V_{tot}{}^* = |V_1|^2 \{1 + |r_2|^2 + |r_3|^2\, |r_2|^2 + 2|r_2|^2\, |r_3| \cdot \cos(\phi_3 + \phi'_3) + \\ + 2|r_2| \cdot \cos(\phi_2 + \phi'_2) + 2|r_2|\, |r_3| \cdot \cos(\phi_2 + \phi'_2 + \phi_3 + \phi'_3)\}.$$

The maximum is reached at $\cos \phi = 1$, so

$$P_M(|r_2|, |r_3|) = P_1 \{1 + |r_2|(1 + |r_3|)\}^2. \qquad (17)$$

With Eq. (17) we can estimate the permissible operating input power $P_M(|r_2|, |r_3|)$ depending on the reflections $|r_2|, |r_3|$ and, with Eq. (18), the nominal value P_{nom} for ($s_2 = 2$ and $s_3 = 1{,}2$):

$$P_M(|r_2|, |r_3|). \frac{1{,}86\, P_{nom}}{1 + |r_2|(1 + |r_3|)^2}. \qquad (18)$$

10 Circulator sizes

The sizes of circulators are governed by two considerations:
- the type of connector used and the operating frequency,
- the maximum power the circulator can handle.

To explain this, let us first consider a small power. Depending on the wavelength, there are various constructions, such as waveguide, stripline and various sizes of connectors. The basic dimensions can differ from type to type, but in principle they must not be below a certain minimum, set by the resonant nature of the structure.

An answer is thus given to the often heard question as to whether small circulators can be built for small powers. Size reduction is possible only as far as the limits set by the principle of operation, unless an entirely different concept is employed, as in lumped-circuit element circulators, where the resonant condition is maintained by external capacitors.

At higher powers the dimensions must of necessity be larger to ensure adequate cooling. The size increase is governed by the convection cooling obtained on the outside of the device, or by thermal contact between the mounting brackets and cooling fins (heatsinks), should these prove necessary.

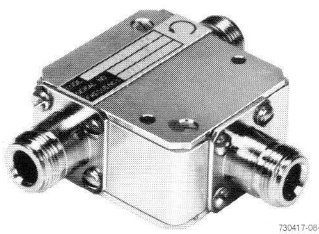

730417-08-01

Coaxial circulator.

11 Magnetic temperature compensation

To illustrate the temperature problems encountered in the development of circulators, some of the special measures taken to compensate for temperature changes in the magnetic circuit of a circulator will be discussed below.

Where only a small operating temperature range is necessary it is possible to use either temperature-compensated microwave ferrites which have a relatively constant maximum magnetic saturation, or microwave ferrites with a linear relationship between temperature and magnetic saturation. By selecting a permanent magnetic material with a suitable temperature coefficient and a suitable shape it is possible to keep the magnetic flux in the microwave ferrite practically constant over a wide temperature range.

These methods fail for circulators which must operate in a considerably wider temperature range. Here additional measures must be taken. By inserting a specially selected compensating material with highly temperature-dependent magnetic saturation in the circulator magnetic circuit, it is possible to expand the temperature range considerably. This method is particularly suitable for low-power circulators in which the h.f. energy dissipation in the microwave ferrite is small.

Fig. 60 shows the construction of a temperature-compensated stripline circulator. Two sections (in this example rings) of the soft-magnetic compensating ferrite are positioned between the microwave ferrite and the permanent magnet.

To keep the compensating ferrite saturated (for only then can the accurately defined temperature-dependent magnetic saturation be used for compensation) it usually has a small cross-sectional area perpendicular to the direction of flow. Soft-magnetic pole pieces are necessary if sufficiently uniform induction over the entire area of the microwave ferrite, the compensating ferrite and the permanent magnet, is to be obtained.

The magnetic circuit, consisting of permanent magnet and compensating ferrite, must be so dimensioned that the induction required for stabilizing the internal field, H_F, can be produced in the microwave ferrite. To arrive at these dimensions it is necessary to calculate the magnetic fluxes and potentials in the circuit, and to determine the dimensions corresponding to the material properties.

During operation, the inherent losses in the microwave ferrite give rise to heat flow from it towards the outer housing by way of the magnets and compensating material. Mechanical means such as air cooling, or loading the permanent magnets with a medium of good thermal conductivity, are used to improve heat removal.

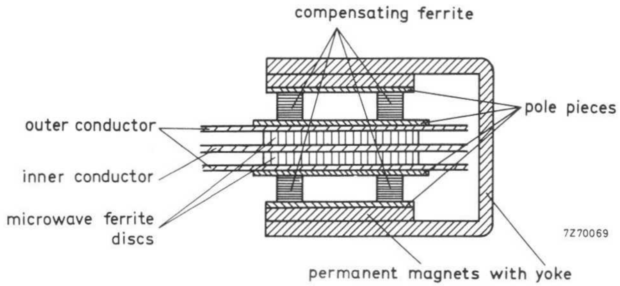

Fig. 60 The constructional features of a temperature-compensated stripline circulator.

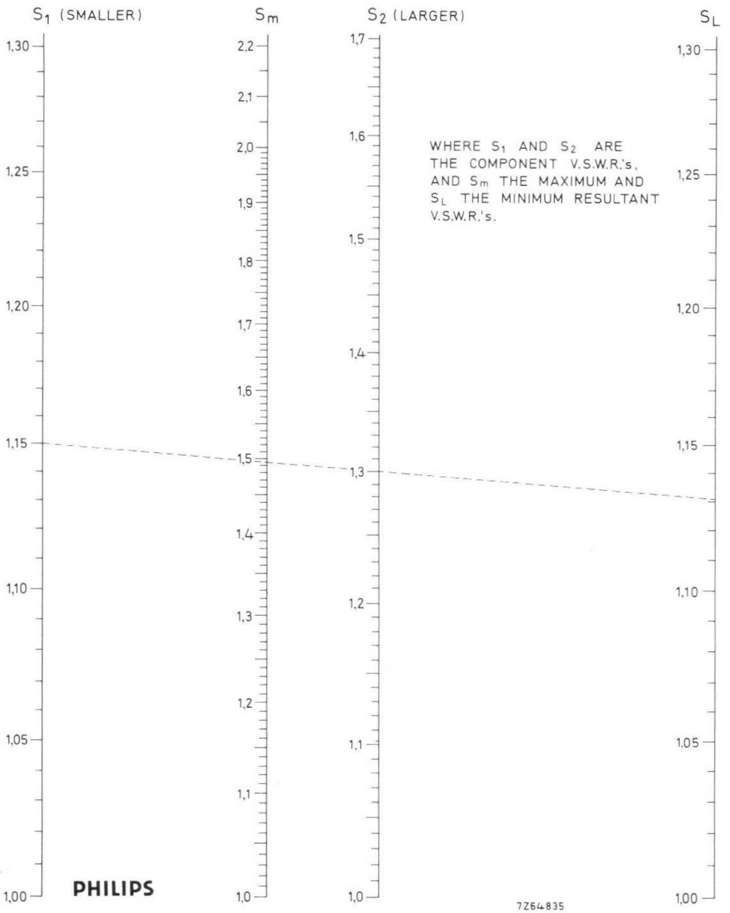

Nomogram showing the maximum and minimum (depending on phase) resultant v.s.w.r. values from two mismatched, cascaded components.

Appendix

Derivation of approximate expressions for the performance of the lossy circulator

The practical circulator is non-reciprocal, but not lossless. It involves as little loss as possible, and is not exactly cyclic-symmetrical (but nearly so). The determination of scattering matrices for a practical circulator would require the use of a *perfectly* accurate measuring facility, and no such facility can exist. However, although a rigorous analysis of lossy circulator performance may not be feasible, some assumptions as to its performance must be made for design purposes and subsequent evaluation, using available measuring equipments and procedures.

In the following paragraphs an approximate analysis is carried out, making the assumptions that the circulator is non-reciprocal, exactly symmetrical, and has low insertion loss and high isolation. This analysis again results in the simplified matrix for the lossless circulator (Eq. 8):

$$\begin{pmatrix} b_1 \\ b_2 \\ b_3 \end{pmatrix} = \begin{pmatrix} S_1, & S_2, & S_3 \\ S_3, & S_1, & S_2 \\ S_2, & S_3, & S_1 \end{pmatrix} \begin{pmatrix} a_1 \\ a_2 \\ a_3 \end{pmatrix} \tag{19}$$

The relationship between the quantities of the matrix elements concerns only the circulator itself, the effects from external circuitry being ignored. If these effects are taken into account, then the practical situation can be described.

Behaviour of a real circulator with mismatched loads

In Section 8.1 the incident wave a_r and the associated reflected wave b_r are defined in terms of the matrix relationship

$$(b) = (S)\,(a).$$

In practice there is only one independent wave incident on port *1*, denoted by a_1 (Fig. 61), although it can of course consist of a mixture of several frequencies and amplitude levels. Waves incident on ports *2* and *3* are only those arising from reflections from the loads with which the ports are terminated. As reflections however, these signals are related to the signals emerging from the same

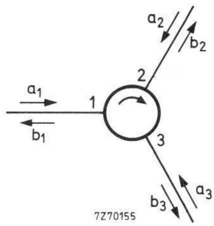

Fig. 61 Incident and emergent wave nomenclature for a circulator.

ports, designated b_2 and b_3. Thus, the waves incident upon ports *2* and *3*, a_2 and a_3, can be written

$$a_2 = S_L\, b_2$$
$$a_3 = S_H\, b_3,$$

where S_L is the reflection coefficient of the load connected to port *2*, and S_H the reflection coefficient of the load connected to port *3*. Substituting these equations in Eq. (19) yields

$$\begin{pmatrix} b_1 \\ b_2 \\ b_3 \end{pmatrix} = \begin{pmatrix} S_1, & S_3, & S_2 \\ S_2, & S_1, & S_3 \\ S_3, & S_2, & S_1 \end{pmatrix} \begin{pmatrix} a_1 \\ S_L b_2 \\ S_H b_3 \end{pmatrix}$$

which expands to give

$$\begin{aligned} b_1 &= S_1 a_1 + S_3 S_L b_2 + S_2 S_H b_3 \\ b_2\,(1 - S_1 S_L) &= S_2 a_1 \qquad\qquad\quad + S_3 S_H b_3 \\ b_3\,(1 - S_1 S_H) &= S_3 a_1 + S_2 S_L b_2. \end{aligned}$$

Solving for b_1, b_2 and b_3 with respect to a_1 yields

$$\frac{b_1}{a_1} = \frac{S_1(1 - S_1S_H - S_1S_L - S_2S_3S_LS_H + S_1{}^2S_HS_L) + S_2S_LS_3(1 - S_1S_H)}{1 - S_1S_H - S_1S_L - S_2S_3S_HS_L + S_1{}^2S_HS_L} +$$

$$+ \frac{S_2S_HS_3(1 - S_1S_L) + S_2{}^3S_HS_L + S_3{}^3S_LS_H}{1 - S_1S_H - S_1S_L - S_2S_3S_HS_L + S_1{}^2S_HS_L} \tag{20}$$

$$\frac{b_2}{a_1} = \frac{S_2(1 - S_1S_H) + S_3{}^2S_H}{1 - S_1S_H - S_1S_L - S_2S_3S_LS_H + S_1{}^2S_HS_L} \tag{21}$$

$$\frac{b_3}{a_1} = \frac{S_3(1 - S_1S_L) + S_2{}^2S_L}{1 - S_1S_H - S_1S_L - S_2S_3S_HS_L + S_1{}^2S_HS_L}. \tag{22}$$

It should be noted that no restriction is imposed on the values of either S_L or S_H which may be anywhere between -1 and $+1$. This implies that a negative-resistance amplifier could be connected to port *2* or to ports *2* and *3* of the circulator.

It should also be noted that, if, by way of a check, in the above equations S_L and S_H are made equal to zero, then the reflection coefficients become $b_1/a_1 = S_1$, $b_2/a_1 = S_2$ and $b_3/a_1 = S_3$, as indeed they should!

Input reflection with low reflection terminations on ports *2* and *3*

Here it is assumed that $|S_2| \approx 1$, and $|S_1|$, $|S_3|$, $|S_H|$, and $|S_L| < 1$; that is to say: S_1, S_3, S_H and S_L are all small and of similar magnitude and it may happen that S_L and S_H approach zero. If Eq. (20) is reconsidered in the light of the above assumptions it can be seen that the numerator is small and of the same order as S_1. When estimating its value it is thus sufficient to take into account values which are small and of the third order. For the denominator, however, it is sufficient to take into account value deviations which are small but of the second order:

$$\frac{b_1}{a_1} \approx \frac{S_1 - S_1{}^2 S_H - S_1{}^2 S_L + S_2 S_L S_3 + S_2 S_H S_3 + S_2{}^3 S_H S_L}{1 - S_1 S_H - S_1 S_L}$$

$$\approx S_1 + S_2 S_L S_3 + S_2 S_H S_3 + S_2{}^3 S_H S_L. \tag{23}$$

An upper limit can then be found by calculating the solutions of each of the component terms:

$$\left|\frac{b_1}{a_1}\right| \approx |S_1| + |S_2| \left(|S_L S_3| + |S_H S_3| + |S_2{}^2 S_H S_L|\right). \tag{24}$$

This relationship applies to symmetrical, lossy circulators. If it can be assumed that circulator losses are zero, then the approximation of Eq. (10) can be used to determine the matrix elements, and, after elimination of S_2 and S_3 (where $|S_2| \approx 1$ and $|S_3| \approx |S_1|$) we arrive at the following expression:

$$|S_1| (1 - |S_L| - |S_H|) - |S_H| |S_L| \leqslant \left|\frac{b_1}{a_1}\right| \leqslant |S_1| (1 + |S_L| + |S_H|) + |S_H| |S_L| \tag{25a}$$

provided that

$$S_1 (1 - |S_L| - |S_H|) - |S_H| |S_L| > 0,$$

if this is not so then the expression becomes

$$0 \leqslant \left|\frac{b_1}{a_1}\right| \leqslant |S_1| (1 + |S_L| + |S_H|) + |S_H| |S_L|. \tag{25b}$$

In this case the absolute value of the externally measured input reflection will lie between the left- and right-hand inequality limits. The numerical conditions for this situation are given in Fig. 62, where it has been assumed that $|S_L| = |S_H|$, which can be the case in practice, for example when similar measuring resistors of the same type are being used. The results show that reflection by the measuring resistors will only have a small effect on the measured value of the input reflection. This means that the input reflection of a circulator can be measured with sufficient accuracy for practical purposes without need of using precision load resistors. As expected, the input reflection differs but little from the ideal, even when ports *2* and *3* are not well matched.

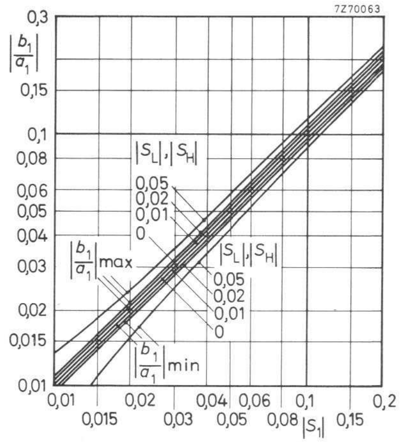

Fig. 62 Limits of Eq. (25*b*), when $|S_L| = |S_H|$.

Input reflection with total reflection at port *2*

Total reflection at port *2* means that $|S_L| = 1$. Taking $|S_1|$, $|S_3|$ and $|S_H| \ll 1$, and $|S_2| \approx 1$, then from the general relationship of Eq. (20) the following expression can be derived:

$$\left|\frac{b_1}{a_1}\right| \approx S_1 (1 + S_2 S_3 + S_2{}^3 S_H) + S_2 S_3 (1 + S_H) + S_2{}^3 S_H. \tag{26}$$

This relationship holds for symmetrical, lossy circulators. If, however, the losses can be taken to be zero, then the approximations given in Eq. (10) for the values of the matrix elements can be used to give:

$$0 \leqslant \frac{b_1}{a_1} \leqslant |S_1| (2 + 2|S_H| + |S_1|) + |S_H|$$

or, approximately, (27)

$$0 \leqslant \left|\frac{b_1}{a_1}\right| \leqslant 2|S_1| + |S_H|.$$

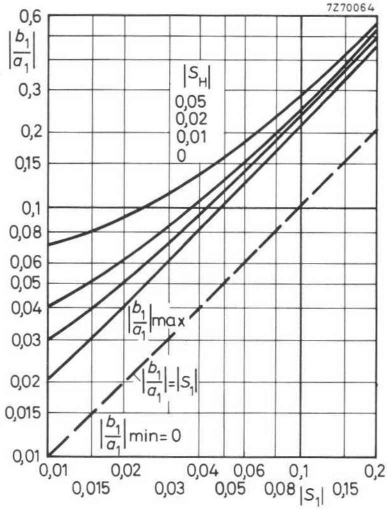

Fig. 63 Graphical solution for Eq. (27).

Practical values have been derived and are given in Fig. 63. It can be seen from this figure, that, even when $S_H = 0$, the user must expect the circulator input reflection seen by the source to be doubled when the load reflects all the power delivered to it. This is of course a reflection coefficient increase of 6 dB. Thus if in some application the maximum permitted input reflection were to be 10%, and allowance had to be made for total reflection from the load, then, the required isolation can be obtained from the return loss nomogram. From Fig. 41 the required v.s.w.r. is 1,21, this corresponds to a return loss of 20 dB, the actual isolation required from the cilculator will thus be $(20 + 6) = 26$ dB.

Input reflection with total reflection at port *3*

Since Eq. (20), is symmetrical with respect to S_L and S_H, the condition of total reflection from port *3* results in a similar expression to that for total reflection from port *2*:

$$0 \leqslant \left|\frac{b_1}{a_1}\right| \leqslant 2|S_1| + |S_L|. \tag{28}$$

If there is no load on port *3*, or if that load is such that it reflects all the energy supplied to it, the observed input reflection will be double that seen under matched conditions, even with a low-reflection termination on port *2*. The values given in Fig. 63 also apply to this situation.

Isolation of a circulator with mismatched loads

General case

The isolation measured between ports *1* and *3* of a circulator with normal external components is nominally:

$$\frac{b_3}{a_1} = \frac{S_3\,(1 - S_1 S_L) + S_2{}^2 S_L}{1 - S_1 S_H - S_1 S_L - S_2 S_3 S_H S_L + S_1{}^2 S_H S_L}. \tag{29}$$

As in the discussion of input reflection, a case of special interest will now be discussed.

Isolation with low reflection terminations on ports 2 and 3

Given that $|S_1|$, $|S_3|$, $|S_H|$ and $|S_L| \ll 1$ and $|S_2| \approx 1$, it follows that:

$$\frac{b_3}{a_1} \approx S_3 + S_2{}^2 S_L + S_2{}^2 S_1\,(S_H + S_L). \tag{30}$$

This relationships holds good for symmetrical lossy circulators.

If the circulator may be assumed to be lossless, it is possible to use the approximations of Eq. (10) for the values of the matrix elements to obtain:

$$|S_3| - |S_L| \leqslant \left|\frac{b_3}{a_1}\right| \leqslant |S_3| + |S_L| \qquad \text{where } |S_L| < |S_3|$$

and (31)

$$|S_L| - |S_3| \leqslant \left|\frac{b_3}{a_1}\right| \leqslant |S_3| + |S_L| \qquad \text{where } |S_L| > |S_3|.$$

Actual values are given in Fig. 64.

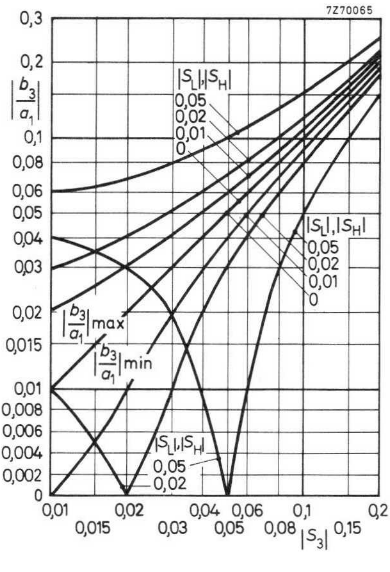

Fig. 64 Values of insertion loss derived from Eq. (31).

Since the values obtained by measurement are strongly influenced by the level of reflection at port 2, it is absolutely necessary to employ precision load resistors when measuring isolation. If precision load resistors are not available, then it should be assumed that $|S_1| = |S_3|$ *because the effect of reflections from* S_L *is small in comparison.*

Relationship between input reflection and isolation with low-reflection terminations at ports *2* and *3*

The question of the deviations between input reflection and insertion loss is of general interest. On the basis of the limiting ellipse considerations concerning only circulators, it follows that $|S_1| \approx |S_3|$. The user will be interested to know how far this still applies when using practical resistors. By means of Eq. 20 and Eq. 22 available for numerator and denominator it is found that

$$\frac{b_1/a_1}{b_3/a_1} = \frac{S_1\,(1 - S_1 S_H - S_1 S_L - S_2 S_3 S_H S_L + S_1{}^2 S_H S_L)}{S_3\,(1 - S_1 S_L) + S_2{}^2 S_L} +$$
$$+ \frac{S_2 S_L S_3\,(1 - S_1 S_H) + S_2 S_H S_3\,(1 - S_1 S_L) + S_2{}^3 S_H S_L + S_3{}^3 S_L S_H}{S_3\,(1 - S_1 S_L) + S_2{}^2 S_L}. \tag{31}$$

Assuming that

$$|S_1|,\ |S_3|,\ |S_H|,\ |S_L| \ll 1;\ |S_2| \approx 1$$

it follows from Eqs (31) and (10) that the ratio between input reflection and isolation equals:

$$\frac{1 - |S_3| - |S_L| - |S_3|\,(|S_L| + |S_H| - |S_3|)}{1 + S|_L|/|S_3|} - |S_H| \leqslant$$
$$\leqslant \left|\frac{b_1/a_1}{b_3/a_1}\right| \leqslant \frac{1 + |S_3| + |S_L| + |S_3|\,(|S_L| + |S_H| + |S_3|)}{1 - |S_L|/|S_3|} + |S_H|. \tag{32}$$

Fig. 65 shows this approximation for ratios where $|S_L| = |S_H|$. With ideal terminations $S_L = 0$ and $S_H = 0$, the range of the ratios of $|b_1/a_1|/|b_3/a_3|$ possible is limited by the following relationship which itself can be derived from the limiting ellipse

$$1 - |S_3| + |S_3|^2 \leqslant \left|\frac{b_1/a_1}{b_3/a_1}\right| \leqslant 1 + |S_3| + |S_3|^2. \tag{33}$$

At about $|S_3| = \sqrt{|S_{L,H}|}$ the set of curves of $|b_1/a_1|/|b_3/a_a| > 1$ have minima of magnitude

$$\left|\frac{b_1/a_1}{b_3/a_1}\right|_{\min} \approx 1 + 2\,|S_3| + 5\,|S_3|^2.$$

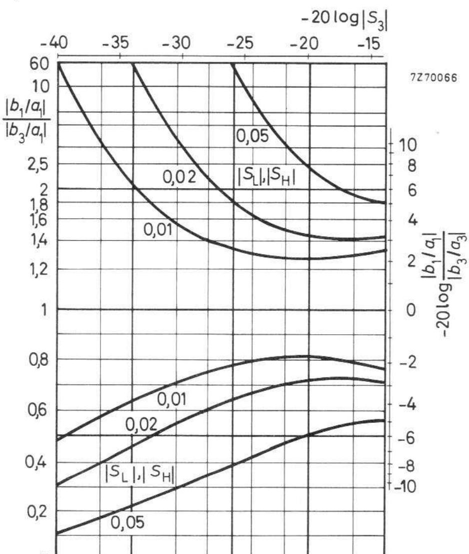

Fig. 65 Calculated approximate ratios between input reflection and isolation, from Eq. (32).

At about $|S_3| = \sqrt{|S_{L,H}|}$ the set of curves of $|b_1/a_1|/|b_3/a_1| < 1$ have their maxima of magnitude

$$\left|\frac{b_1/a_1}{b_3/a_1}\right|_{\max} \approx 1 - 2\,|S_3| + |S_3|^2.$$

The graph in Fig. 65 shows that *even with ideal terminations*, discrepancies of several dB can occur between the measured results of input reflection and isolation. With a circulator having a measured isolation of, say, 20 dB (i.e. $|S_3| = 0{,}1$) and terminated with resistors that reflect no more than 1 %, the measured logarithmic input reflection can still vary about $\pm$ 2 dB.

As explained already, the main uncertainty factor lies in the isolation measurement. To arrive at a satisfactory agreement, the measurement must be made with high-quality precision resistors. Even under ideal conditions the discrepancies described by the limiting ellipse are still likely to occur.

Insertion loss

General case

The general expresssion for the insertion loss between any two ports of a circulator is:

$$\frac{b_2}{a_1} = \frac{S_2\,(1 - S_1 S_H) + S_3{}^2 S_H}{1 - S_1 S_H - S_1 S_L - S_2 S_3 S_L S_H + S_1{}^2 S_H S_L}\,. \tag{34}$$

Insertion loss with low reflection terminations on ports 2 and 3

Here it is assumed that $|S_1|$, $|S_3|$, $|S_L|$ and $|S_H| \ll 1$, and that $|S_2| \approx 1$. It then follows that

$$|S_2|\,(1 - |S_1|\,|S_L|) \leqslant \left|\frac{b_2}{a_1}\right| \leqslant |S_2|\,(1 + |S_1|\,|S_L|). \tag{35}$$

provided that the right-hand term is less than unity. Here, the relationship $|S_2| \approx 1 - |S_1|^2$ derived from Eq. (10) must not be used to determine $|S_2|$, but $|S_2|$ must be regarded as the actual insertion loss, consisting of the inherent loss of the circulator plus the various reflection losses. When the insertion losses are low, the upper limit of the right-hand term of Eq. (33) may be greater than nuity, which is too high; for Eq. (33) to hold, b_2/a_1 must be less than unity.

With normally occurring values it is possible to detemine the insertion losses with greater accuracy by shifting the phase of the load reflection, that is making $|S_L| = \pm |S_L|$ and by averaging. It is thus possible, means of a well-compensated phase shifter, to establish that:

$$S_2 = \frac{|b_2/a_1|_{\max} + |b_2/a_1|_{\min}}{2}$$

when $|S_1|$, $|S_3|$ and $|S_H| \ll 1$, and $S_L = 1$.

Bibliography

[1] Polder, D., On the theory of electromagnetic resonance, Phil. Mag. 40 (1949), p. 99.

[2] Fay, C. E. and Comstock, R. L., Operation of the ferrite junction circulator, IEEE trans. MTT-13, January 1965.

[3] Bosma, H., On stripline Y-circulation at UHF, IEEE trans. MTT-12 January 1964, pp. 61-72.

[4] Butterweck, H. J., Der Y-Zirculator, AEU 17 (1963), p. 163.

Argentina
FAPESA I.y.C.
Av. Crovara 2550
Tel. 652-7438/7478
BUENOS AIRES

Australia
Philips Industries Ltd.
Elcoma Division
67-71 Mars Road
Tel. 42 1261
LANE COVE, 2066, N.S.W.

Austria
Österreichische Philips
Bauelemente Industrie G.m.b.H.
Zieglergasse 6
Tel. 93 26 22
A1072 VIENNA

Belgium
M.B.L.E
80, rue des Deux Gares
Tel. 23 00 00
1070 BRUSSELS

Brazil
IBRAPE S.A.
Av. Paulista 2073-S/Loja
Tel. 278-1111
SAO PAULO, SP.

Canada
Philips Electron Devices
116, Vanderhoof Ave.
Tel. 425-5161
TORONTO 17, Ontario

Chile
Philips Chilena S.A.
Av. Santa Maria 0760
Tel. 39-40 01
SANTIAGO

Colombia
SADAPE S.A.
Calle 19, No. 5-51
Tel. 422-175
BOGOTA D.E. 1

Denmark
Miniwatt A/S
Emdrupvej 115A
Tel. (01) 69 16 22
DK-2400 KØBENHAVN NV

Finland
Oy Philips Ab
Elcoma Division
Kaivokatu 8
Tel. 17271
SF-00100 HELSINKI 10

France
R.T.C.
La Radiotechnique-Compelec
130 Avenue Ledru Rollin
Tel. 355-44-99
PARIS 11

Germany
Valvo G.m.b.H.
Valvo Haus
Burchardstrasse 19
Tel. (040) 3296-1
2 HAMBURG 1

Greece
Philips S.A. Hellénique
Elcoma Division
52, Av. Syngrou
Tel. 915 311
ATHENS

Hong Kong
Philips Hong Kong Ltd.
Components Dept. (Kowloon Branch)
7th Fl., Wai Yip Industrial Building
41 Tsun Yip St., Kwuntong
Tel. K-42 72 32
HONG KONG

India
INBELEC Div. of
Philips India Ltd.
Band Box House
254-D, Dr. Annie Besant Road
Tel. 457 311 to 15
Prabhadevi, BOMBAY-25-DD

Indonesia
P.T. Philips-Ralin Electronics
Elcoma Division
Djalan Gadjah Mada 18
Tel. 44 163
DJAKARTA

Ireland
Philips Electrical (Ireland) Ltd.
Newstead, Clonskeagh
Tel. 69 33 55
DUBLIN 14

Italy
Philips S.p.A.
Sezione Elcoma
Piazza IV Novembre 3
Tel. 69 94
MILANO

Japan
NIHON PHILIPS
32nd Fl. World Trade Center Bldg.
5, 3-chome, Shiba Hamamatsu-cho
Minato-ku
Tel. (435) 5204-5
TOKYO

Mexico
Electrónica S.A. de C.V.
Varsovia No. 36
Tel. 5-33-11-80.
MEXICO 6, D.F.

Netherlands
Philips Nederland B.V.
Afd. Elonco
Boschdijk 525
Tel. (040) 79 33 33
EINDHOVEN

New Zealand
EDAC Ltd.
70-72 Kingsford Smith Street
Tel. 873 159
WELLINGTON

Norway
Electronica A.S.
Middelthunsgate 27
Tel. 46 39 70
OSLO 3

Peru
CADESA
Jr. Ilo, No. 216
Appartado 10132
Tel. 27 7317
LIMA

Philippines
EDAC
Philips Industrial Dev. Inc.
2246 Pasong Tamo Street
Tel. 88-94-53 (to 56)
MAKATI-RIZAL

Portugal
Philips Portuguesa S.A.R.L.
Av. Eng. Duharte Pacheco 6
Tel. 68 31 21
LISBOA 1

Singapore
Philips Singapore Private Ltd.
Elcoma Div.,
P.O. Box 340, Toa Payoh Central P.O.,
Lorong 1, Toa Payoh
Tel. 53 88 11
SINGAPORE 12

South Africa
EDAC (Pty.) Ltd.
South Park Lane
New Doornfontein
Tel. 24/6701-2
JOHANNESBURG

Spain
COPRESA S.A.
Balmes 22
Tel. 329 63 12
BARCELONA 7

Sweden
ELCOMA A.B.
Lidingövägen 50
Tel. 08/67 97 80
10250 STOCKHOLM 27

Switzerland
Philips A.G.
Edenstrasse 20
Tel. 01/44 22 11
CH-8027 ZUERICH

Taiwan
Philips Taiwan Ltd.
San Min Building, 3rd Fl.
57-1, Chung Shan N. Road
Section 2
P.O. Box 22978
Tel. 553101-5
TAIPEI

Turkey
Türk Philips Ticaret A.S.
EMET Department
Gümüssuyu Cad. 78-80
Tel. 45.32.50
Beyoglü, ISTANBUL

United Kingdom
Mullard Ltd.
Mullard House
Torrington Place
Tel. 01-580 6633
LONDON WC1E 7HD

United States
North American Philips
Electronic Component Corp.
230, Duffy Avenue
Tel. (516) 931-6200
HICKSVILLE, N.Y. 11802

Uruguay
Luzilectron S.A.
Rondeau 1567, piso 5
Tel. 9 43 21
MONTEVIDEO

Venezuela
C.A. Philips Venezolana
Elcoma Department
Av. Principal de los Ruices
Edif. Centro Colgate
Apartado 1167
Tel. 36.05.11
CARACAS

Printed in The Netherlands 12-74 9399 466 03401